2018년 2월
석사학위 논문

Study of natural compounds isolated from the stem of *Fatsia japonica* on the regulation of anti-inflammatory and neuro-protective effects

조선대학교 대학원

약 학 과

이 환

Study of natural compounds isolated from the stem of *Fatsia japonica* on the regulation of anti-inflammatory and neuro-protective effects

팔손이 줄기에서 분리한 천연화합물들의
항염증 및 뇌세포 보호효과 조절 연구

2018년 2월 23일

조선대학교 대학원

약 학 과

이 환

Study of natural compounds isolated from the stem of *Fatsia japonica* on the regulation of anti-inflammatory and neuro-protective effects

지도교수 이 동 성

이 논문을 약학 석사학위신청 논문으로 제출함

2017년 10월

조선대학교 대학원

약 학 과

이 환

이환의 석사학위논문을 인준함

위원장 조선대학교 교 수 우 은 란 (인)

위 원 조선대학교 교 수 홍 준 희 (인)

위 원 조선대학교 교 수 이 동 성 (인)

2017년 11월

조선대학교 대학원

Contents

Contents i

List of Scheme iii

List of Figures iv

List of Abbreviations vi

국문 초록 viii

Abstract x

1. Introduction 1

1.1. *Fatsia japonica* 1

1.2. Neurodegenerative diseases & Inflammation 3

1.3. General information of neuronal cell lines 6

1.3.1. Mouse hippocampal HT22 cells 6

1.3.2. Murine microglia BV2 cells 7

2. Materials and Methods 10

2.1. Materials 10

2.1.1. Plant Material 10

2.1.2. Chemicals, reagents and chromatography for isolation 10

2.1.3. Chemicals and reagents for cell culture 11

2.2. Method 11

2.2.1. General experimental procedures 11

2.2.2. Extraction and Isolation 12

2.2.2.1. Extraction 12

2.2.2.2. Isolation 13

2.2.2.2.1. Isolation of fraction FJB 13

2.2.2.2.2. Isolation of fraction FJBS 14

2.2.2.2.3. Isolation of fraction FJBH 15

2.2.2.2.4. Isolation of fraction FJBN 16

2.2.3. Structure identification of compounds 17

2.2.4. Cell culture 24

2.2.5. MTT assay.....24

2.2.6. Nitrite Assay 24

2.2.7. Western blot analysis 24

2.2.8. PGE_2 Assay.....25

2.2.9. Statistical Analysis 25

3. Results and Discussion 26

3.1. The biological effects of fractions from *Fatsia japonica* extracts. 26

3.1.1. The effects of fractions from *Fatsia japonica* extracts on cell viability and nitrite reduction in RAW264.7 cells.....27

3.1.2. The effects of fractions from *Fatsia japonica* extracts on cell viability and nitrite reduction in BV2 cells. 32

3.1.3. The effects of fractions from *Fatsia japonica* extracts on cell viability by MTT assay in HT22 cells. 37

3.2. Structure determination of isolated compounds from *Fatsia japonica* 40

3.2.1. Compound 1 40

3.2.2. Compound 2 42

3.2.3. Compound 3 44

3.2.4. Compound 4 46

3.3. The anti-inflammatory, anti-neuroinflammatory and neuro-protective action by compounds 1-4from *Fatsia japonica* 48

3.3.1. The effect of compounds1-4from *Fatsia japonica* on cell viability and nitrite reduction in RAW264.7 cells. 49

3.3.2. The effect of compounds 1-4from *Fatsia japonica* on cell viability and nitrite reduction in BV2 cells. 50

3.3.3. The effect of compounds 1-4from *Fatsia japonica* on cell viability by MTT assay in HT22 cells. 51

4. Colclusion 52

5. Reference 54

Appendix 58

감사의 글 75

List of Schemes

Scheme 1: Extraction and fraction from *Fatsia japonica* Stem 12

Scheme 2: Isolation of fraction FJB1-10 from *n*-BuOH fraction of Fatsia japonica Stem 13

Scheme 3: Isolation of fraction FJBS1-14 from *n*-BuOH fraction of *Fatsia japonica* Stem 14

Scheme 4: Isolation of fraction FJBH1-7 from *n*-BuOH fraction of *Fatsia japonica* Stem 15

Scheme 5: Isolation of fraction FJBN1-7 from *n*-BuOH fraction of *Fatsia japonica* Stem 16

List of Figures

Fig.1: *Fatsia japonica*; Leaves, flowers, and trees 2

Fig.2: Oxidative Stress & neuroinflammation 5

Fig.3: Cell biological approach using neuronal cell lines 8

Fig.4: Mouse hippocampal HT22 cells & murine microglia BV2 cells 9

Fig.5: The effect of MeOH extracts from *Fatsia japonica* on nitrite reductionin RAW264.7 cells. 28

Fig.6: The effect of MeOH extracts from *Fatsia japonica* on prostaglandin E2(PGE_2) reduction in RAW264.7 cells. 29

Fig.7: The effects of MeOH extracts from *Fatsia japonica* on inducible nitric oxide synthase (iNOS) and cyclooxygenase-2 (COX-2) expression in RAW264.7 cells. ...30

Fig.8: The effects of fractions from *Fatsia japonica* on nitrite reduction in RAW264.7 cells. 31

Fig.9: The effects of MeOH extracts from *Fatsia japonica* on nitrite reduction in BV2 cells. 33

Fig.10: The effects of MeOH extracts from *Fatsia japonica* on prostaglandin E2 (PGE_2) reduction in BV2 cells. 34

Fig.11: The effects of MeOH extracts from *Fatsia japonica* on inducible nitric oxide synthase (iNOS) and cyclooxygenase-2 (COX-2)expression in BV2 cells. 35

Fig.12: The effects of fractions from *Fatsia japonica*on nitrite reduction in BV2 cells. 36

Fig.13: The effects of MeOH extracts from *Fatsia japonica* on cell viability by MTT assay in HT22 cells. 38

Fig.14: The effects of fractions from *Fatsia japonica* on cell viability by MTT assay in HT22 cells. 39

Fig.15: Structures of compound 1 from *n*-BuOH fraction of *F. japonica*. 41

Fig.16: Structures of compound 2 from *n*-BuOH fraction of *F. japonica*. 43

Fig.17: Structures of compound 3 from *n*-BuOH fraction of *F. japonica*. 45

Fig.18: Structures of compound 4 from *n*-BuOH fraction of *F. japonica*. 47

Fig.19: The effects of compounds 1-4 from *Fatsia japonica* on nitrite reduction in RAW264.7 cells. 49

Fig.20: The effects of compounds 1-4 from *Fatsia japonica* on nitrite reduction in BV2 cells.....50

Fig.21: The effects of compounds 1-4 from *Fatsia japonica* on cell viability by MTT assay in HT22 cells. 51

Fig.22: ^{1}H-NMR spectrum of compound 1 (500 MHz, DMSO-D_6) 59

Fig.23: ^{13}C-NMR spectrum of compound 1 (500 MHz, DMSO- D_6) 60

Fig.24: HSQC spectrum of compound 1 (500 MHz, DMSO- D_6).....61

Fig.25: HMBC spectrum of compound 1 (500 MHz, DMSO- D_6).....62

Fig.26: ^{1}H-NMR spectrum of compound 2 (500 MHz, DMSO- D_6) 63

Fig.27: ^{13}C-NMR spectrum of compound 2 (500 MHz, DMSO- D_6) 64

Fig.28: HSQC spectrum of compound 2 (500 MHz, DMSO- D_6).....65

Fig.29: HMBC spectrum of compound 2 (500 MHz, DMSO- D_6).....66

Fig.30: ^{1}H-NMR spectrum of compound 3 (500 MHz, DMSO- D_6) 67

Fig.31: ^{13}C-NMR spectrum of compound 3 (500 MHz, DMSO- D_6) 68

Fig.32: HSQC spectrum of compound 3 (500 MHz, DMSO- D_6).....69

Fig.33: HMBC spectrum of compound 3 (500 MHz, DMSO- D_6).....70

Fig.34: ^{1}H-NMR spectrum of compound 4 (500 MHz, DMSO- D_6) 71

Fig.35: ^{13}C-NMR spectrum of compound 4 (500 MHz, DMSO- D_6) 72

Fig.36: HSQC spectrum of compound 4 (500 MHz, DMSO- D_6).....73

Fig.37: HMBC spectrum of compound 4 (500 MHz, DMSO- D_6).....74

List of Abbreviations

***F. japonica*:** *Fatsia japonica*

AD: Alzheimer's disease

CNS: Central nervous system

MIP2: Markedly macrophage inflammatory protein-2

IL-6: Interleukin-6

NO: Nitric oxide

TNF *α*: Tumor necrosis factor-alpha

iNOS: Inducible nitric oxide synthase

COX-2: Cyclooxygenase-2

PGE_2: Prostaglandin E2

H_2O_2: Hydrogen peroxide

LPS: Lipopolysaccharide

m/z: Mass to charge ratio

MW: Molecular weight

ppm: Parts per million

RP: Reverse phase

NP: Normal phase

C.C.: Column chromatography

UV: Ultraviolet absorption

IR: Infrared spectroscopy

NMR: Nuclear magnetic resonance

MS: Mass spectrum

EIMS: Impact mass spectroscopy

HREIMS: High resolution electro impact mass spectroscopy

HPLC: High performance liquid chromatography

TLC: Thin layer chromatography

***J*:** Spin-spin coupling constant [Hz]

m: Multiplet (in connection with NMR data)

s: Singlet

t: Triplet

br: Broad

MHz: Mega hertz

MPLC: Medium pressure liquid chromatography

LPLC: Low pressure liquid chromatography

COSY: Correlation spectroscopy

HSQC: Heteronuclear Single Quantum Coherence

HMBC: Heteronuclear Multiple Bond Correlation

PBS: Phosphate-buffered saline

FBS: Fetal bovine serum

NaCl: Sodium Chloride

KCl: Potassium Chloride

CD spectra: Circular dichroism

KBSI: Korea Basic Science Institute

FD-MS: Field desorption mass spectrometry

^{1}H NMR: Proton NMR

^{13}C NMR: Carbon NMR

CD_3OD: Deuterated methanol

DMSO-D_6: Dimethyl sulfoxide-D_6

DMSO: Dimethyl sulfoxide

DMEM: Dulbecco's Modified Eagle's Medium

Alpha-MEM: Minimum Essential Medium Eagle - alpha modification

RPMI: Roswell Park Memorial Institute

MTT: 3-(4,5-dimethylthiazol-2-yl)-2,5-diphenyltetrazolium bromide

국문 초록

팔손이(*Fatsia japonica*) 줄기에서 분리한 천연화합물들의 항염증 및 뇌세포 보호효과 조절 연구

이 환
지도교수 : 이 동 성
약학과
조선대학교 대학원

팔손이(*Fatsia japonica*)는 두릅나무과(Araliaceae)에 속하는 관목으로 이명으로는 팔각금반(八角金盤)이라 불리는 여러해살이 식물이다. 두릅나무과의 특징은 흔히 줄기에 가시가 있으며 꽃은 산형화서로 달리고, 하위자방의 각 실에 1개의 배주가 들어있고 열매는 장과 또는 핵과이며, 팔손이와 함께 두릅나무(Aralia), 오갈피(Acanthopanax), 황칠나무(Dendropanax), 음나무(Kalopanax), 인삼(panax) 등이 두릅나무과에 속해있다. 또한 선행연구에 의하면 60~80속 정도의 범위가 설정되어 있으며, 약 900종이 주로 열대와 아열대를 중심으로 분포하고 있는 것으로 알려져 있다. 국내에는 8속 14종 5변종 1품종이 자생하는 것으로 알려져 있다. 팔손이의 자생지는 한국,일본 및 대만 등 동아시아 지역에 분포하며 우리나라에서는 제주도를 비롯한 경상남도 및 전라남도 등 남부 지방의 해안가 근처에 자라는 상록활엽수 관목이다. 팔손이의 특징은 잎의 양 면에 털이 없고 표면은 짙은 녹색으로 윤태가 있으며, 뒷면은 황록색을 띄며 직사광선에 잎이 상하므로 그늘진 곳에서 잘 자란다. 팔손이의 키는 1~3m이며, 둥근 잎은 어긋나나 가지 끝에서는 긴 잎자루 끝에 뭉쳐나는데, 잎의 길이는 20~40cm로 매우 크고 잎몸이 7~9개로 크게 갈라져 손바닥을 편 모양을 나타내어 팔손이라고 부른다. 팔손이는 관상용 식물로 알려져 있으며 팔손이 잎을 통한 약리작용으로는 진해, 거담, 동통, 요통, 류마티

스에 효과가 있다고 알려져 있다. 또한 선행연구에 의해 분리 및 보고된 팔손이의 성분은 fatsioside A, palmitic acid, adenosine, oleanolic acid, hederagenin, acacetin, arabinopyranoside, isovitexin, astragalin, quercetin 등으로 알려진 상태이다. 그러나 팔손이는 관상용 식물로 널리 알려진 만큼 활성성분분리 및 생리활성에 대한 선행연구는 미미한 상태이다. 또한 보고된 약리작용이 대부분 잎을 통해 작용되는 것으로 알려져 있으며 잎에는 독성물질인 fatsiasapotoxin, α-fatsin, β-fatsin이 있는 것으로 알려져 있다. 팔손이를 선정하게 된 배경은 조선대학교 약초원으로부터 팔손이를 비롯한 원식물 총 47종을 채취하여 각각의 식물에 대한 총 217개의 추출물(47개) 및 분획물(170개)를 분획과정을 통해 얻은 후 HT22 해마세포, BV2 미세아교세포, RAW264.7 대식세포를 이용한 활성탐색을 통해 항염증 및 뇌세포 보호효과를 확인하였으며, 그 중 항염증 및 뇌세포 보호효과에 긍정적인 활성을 나타내며 선행연구가 많이 되지 않은 팔손이를 선택하였다. 두릅나무과의 특성상 약리성분이 주로 뿌리껍질, 줄기껍질에 분포하고 있다고 보고되어 있으며 현재 팔손이의 줄기에 대한 분석이 미미하므로 본 연구에서는 팔손이 잎이 아닌 줄기(Stem)부위를 추출 및 분획과정을 거쳐 얻어진 추출물, 클로로포름, 에틸아세테이트, 부탄올, 물층 총 5개의 추출물 및 분획물에 대한 항염증 및 뇌세포 보호효과 조절 비교연구를 실행하여 긍정적인 활성효과 및 양이 가장 많은 부탄올 분획물을 선택하였다. 활성성분 분리를 시도하기 위해 팔손이 줄기 부탄올 분획물을 LPLC, MPLC, 실리카겔, HP20, sepadex, mci-gel 컬럼 크로마토그래피를 통해 다양한 용매조건을 사용하여 반복적으로 실험한 결과 4개의 화합물을 분리하였다. 각각의 팔손이 줄기 유래 화합물 1-4는 ^{1}H-NMR, ^{13}C-NMR, H-^{1}HCOSY, HSQC, HMBC 분광분석 등의 1D 및 2D NMR에 기초하여 maltose (**1**), begoniifolide A (**2**), leiyemudanoside B (**3**), leonticin F (**4**)로 구조결정 하였으며, 4개의 화합물에 대한 항염증 억제, 뇌염증억제 및 뇌세포 보호효과를 확인하였다. 본 연구에서는 팔손이 줄기에 내재되어있는 천연화합물을 발견하고 또한 팔손이 줄기 유래 추출물, 분획물, 단일 화합물들에 대해 처음으로 항염증 억제, 뇌염증억제 및 뇌세포 보호효과 조절 연구를 확인하였다.

Abstract

Study of natural compounds isolated from the stem of *Fatsia japonica* on the regulation of anti-inflammatory and neuro-protective effects

Lee, Hwan

Advisor: Prof. Lee, Dong-Sung

College of Pharmacy

Graduate School of Chosun University

Fatsia japonica (F. japonica) is a shrub belonging to the Araliaceae, and is a perennial plant called a pal-gak-geum-ban. Representative plants belonging to Araliaceae with *F. japonica* include *Acanthopanax, Dendropanax, Kalopanax,* and *Panax*. The characteristics of Araliaceae are mostly thorn on the stem, flowers are umbel shape and the fruit is a bowel or a nucleus. According to previous researches, the range of about 60 ~ 80 genus has been established, and about 900 species are mainly distributed around tropical and subtropical locations. In Korea, 8 genus and 14 species are known to be grow wild. The *F. japonica* is grown wild to eastern Asia, including Korea, Japan, and Taiwan. In Korea, they are evergreen broad-leaved shrubs that grow near the coasts of southern provinces such as Jeju Island, Gyeongsangnamdo and Jeollanamdo. It has no hairs on both sides of the leaf; it has dark green color, and has a yellowish green color on the back side. Also, leaves grow in shady places because they are damaged by direct sunlight. The height of *F. japonica* is 1 ~ 3m, the length of leaf is 20 ~ 40cm and it is very large and leaf blades are 7 ~ 9 large. *F japonica* is known as ornamental plant, and it is also known that pharmacological action through *F. japonica* leaf is effective for asthma, antitussive, expectorant, ache, gout and rheumatism and so on. According to previous studies, various components such as fatioside A, palmitic acid, adenosine, oleic acid, hydergen, acacetin, arabinopyranoside, isobutyricin, astragalin and quercetin has been reported as components separated from *F. japonica*. It is also known that most of the reported

pharmacological actions are through the leaves, and the leaves are known to contain toxic compounds fatsia-sapotoxin, α-fatsin and β-fatsin. In the previous studies, *F. japonica* is well known as ornamental plants, but there are no studies about the anti-inflammatory, anti-neuroinflammatory, and neuro-protective actions of components from *F. japonica*. To explain about the selected background of *F. japonica*, firstly 47 species of plants including *F. japonica* were collected from Chosun University herb garden. And I got total extracts (47) and fractions (170). Next, I have checked the anti-inflammatory, anti-neuroinflammatory, and neuro-protective effects of extracts and fractions from all 47 species of plants. Finally, I selected *F. japonica* with consideration about biological activities and amount of yield. In order to isolate the components from *F. japonica*, I have isolated **4** compounds by LPLC, MPLC, silica gel, HP-20, sephadex, and MCI-gel column chromatography with repeatedly using various solvent systems. Compounds **1**-**4** structure were determined based on 1D and 2D NMR such as ^{1}H-NMR, ^{13}C-NMR, ^{1}H-^{1}HCOSY, HSQC and HMBC spectroscopy as maltose (**1**), begoniifolide A (**2**), leiyemudanoside B (**3**), leonticin F (**4**). I have also confirmed the anti-inflammatory, anti-neuroinflammatory, and neuro-protective effects of compounds **1**-**4**. In this thesis, it is first time experiments on the anti-inflammatory, anti-neuroinflammatory, and neuro-protective actions of extracts, fraction, and **4** natural compounds isolated from *F. japonica* stem.

1. Introduction

1.1. *Fatsia japonica*

Fatsia japonica is a shrub belonging to Araliaceae [1]. Features of Araliaceae is often thorns on the stems, flower are umbel, contains one ovule in each compartment of the inferior ovary and fruits are berries or drupe, it belongs to Araliaceae with *F. japonica* and *Aralia, Acanthopanax, Dendropanax, Kalopanax, Panax* and so on. According to previous researches, the range of 60 ~ 80 genus has been established, and about 900 species are mainly distributed in tropical and subtropical regions. In Korea, 8 genus, 14 species, 5 variety, 1 forma are known to naturally grow. The native species of *F. japonica* is a sub-tropical plant distributed in Korea, Japan, and Taiwan. In Korea, it is an evergreen broad-leaved shrub that grows near Jeju-do, Gyeongsangnam-do and Jeollanam-do. The *F. japonica* has no hairs on both sides of the leaf, the surface is dark green with gloss, the back side is yellowish green, and the leaves are damaged in direct sunlight, so it grows well in shady places [2]. The height of *F. japonica* is 1 ~ 3m, the length of leaf is 20 ~ 40cm and it is very large and leave blades are 7 ~ 9 large and divide into palms, called *F. japonica*. It is known that *F. japonica* is known as an ornamental plant and contains hemolytic and toxic components [3, 4]. In addition pharmacological action through *F. japonica* leaves is known to be effective for asthma, antitussive, expectorant, ache, gout and rheumatism. The major components of *F. japonica* by previous studies are known as fatsioside A, palmitic acid, adenosine, oleanolic acid, hederagenin, acacetin, astragalin, quercetin and so on [5- 7]. In the previous studies, *F. japonica* is well known as ornamental plants, but there are rare studies about the anti-inflammatory, anti-neuroinflammatory, and neuro-protective actions of components from *F. japonica*.

Fig. 1: *Fatsia japonica*; Leaves, Flowers, trees [8].

1.2. Neurodegenerative diseases & Inflammation

Neurodegenerative disease is a brain-related disease that occurs as get aged. Until now, due to unknown causes, the specific brain cell group of the brain and spinal cord gradually lose its function, the number of brain cells decreases, the death of brain cells most important for information transmission of the brain nervous system, the information between brain cells and brain cells, which is known to be caused by the formation of synapses or functional problems, and by the ideal symptom or reduction of the electroencephalography of the brain [9]. According to Korea's aging population, in 1960, the elderly population aged 65 or older was 2.9% of the total population, but in 2000 it reached 7.1% and entered the age of aging, and it is expected to exceed 14% in 2022. Due to the rapid progress of the aging society, the rate of the development of neurodegenerative diseases is also increasing rapidly, and the social burden is also reaching serious level. Compared to the West, where the social security system is well established, Korea has a poor environment, which requires individuals to shoulder the burden entirely. Thus, early diagnosis and treatment of dementia is the best way to reduce the burden of many aspects, both personally and socially. Neurodegenerative diseases are classified into Alzheimer's disease (AD), Parkinson's disease, Huntington's disease, Lou Gehrig's disease and so on according to the main symptom and the affected brain area [10]. The characteristic of neurodegenerative diseases is the death of nerve cells, and it is important to reduce the damage caused by nerve cell death [11]. Until now, the researchers have focused on cell death caused by chronic activation and oxidative stress of neuroinflammation mediated by microglial cells and central nervous system (CNS) macrophages, which have been shown to increase the risk of neurodegeneration [12]. Oxidative stress and excessive inflammatory responses in

the CNS are known to be associated with a variety of neurodegenerative diseases including AD [13].

Prolonged inflammation can cause to a variety of diseases, including arthritis, neurodegenerative disorders, inflammatory bowel disease and septic shock syndrome. An enormous inflammatory response also causes an interruption of tissue functions and can lead to disease pathogenesis [14]. Exposure of immune cells, including macrophages, to particular agonist activates complex signaling cascades that immediately trigger production of chemokines and pro-inflammatory cytokines, markedly macrophage inflammatory protein-2 (MIP2), interleukin-6 (IL-6), nitric oxide (NO), tumor necrosis factor-alpha (TNF α), inducible nitric oxide synthase (iNOS), and cyclooxygenase-2 (COX2), plays a crucial role of commencing inflammatory response [15- 17].

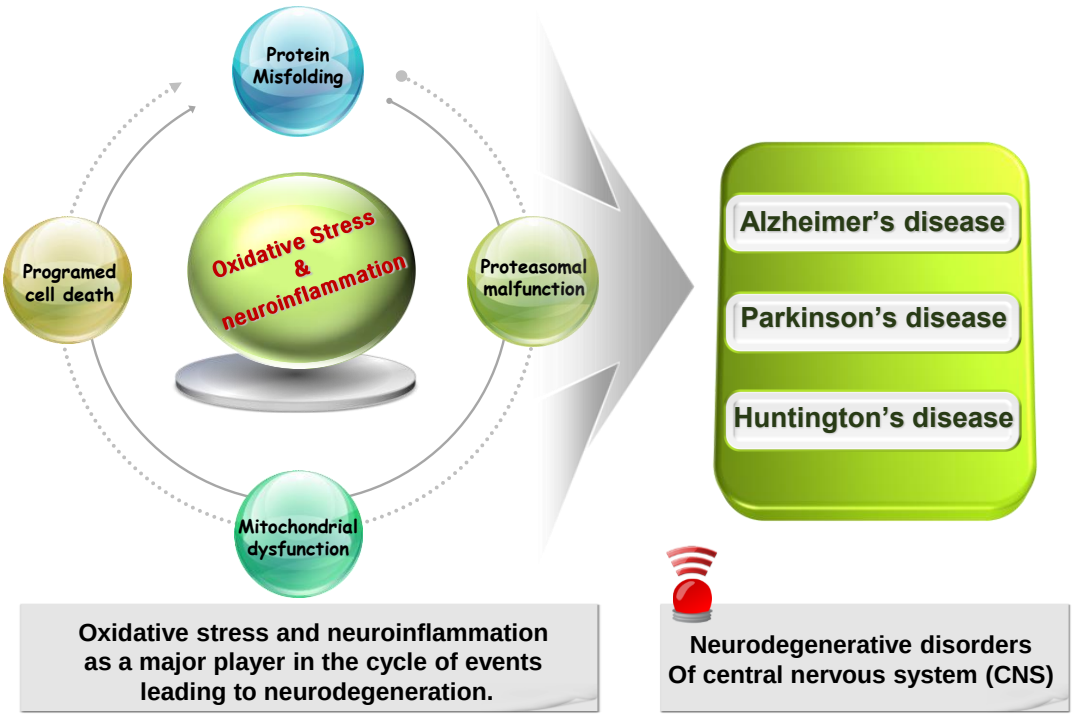

Fig. 2: Oxidative Stress & neuroinflammation

1.3. General information of neuronal cell lines

1.3.1. Mouse hippocampal HT22 cells

The neuronal damages caused by overstimulated excitatory receptors, known as excitotoxicity, have been involved in many neurological disorders [18]. Glutamate is the important excitatory neurotransmitter and plays key roles in brain development and processes related to the movement control, memory, and learning in the CNS [19]. However, the overstimulation of glutamate receptors has been involved in the neuronal damage observed in many neurodegenerative diseases [20, 21]. The neuronal HT22 cell line originated from the mouse hippocampus lacks glutamate receptors, therefore it can cause for glutamate mediated cell death [22]. Hydrogen peroxide (H_2O_2) is a major cause of free radicals and is continually produced from their metabolic activity within the body. If H_2O_2 is accumulated in the cells, it is converted to molecules which can cause cell injury irreversibly [23]. Some enzymes such as glutathione peroxidases and catalase are able to detoxify the formed H_2O_2 in the cells. On the other hand, some neuronal cells show lower catalase levels, therefor, the burden falls on the glutathione pathway [24].

1.3.2. Murine microglia BV2 cells

Microglial cells function as the immune cells of the CNS, acting as primary mediators of inflammation. In response to some negative stimulus such as a free radicals and tissue or organ damages, microglial cells presume a reactive state characterized by the widening and shortening of microglial processes [25]. Activated microglia can produce glutamate transporters and antioxidants to promote correct neuronal function. However, activated microglia are also able to generate several neurotoxic compounds including NO and several pro-inflammatory cytokines that are associated with neurological diseases and CNS disturbances [26, 27]. In CNS inflammation, microglial responses and activation can be mediated from various agents, including lipopolysaccharide (LPS) and several pro-inflammatory cytokines [28, 29].

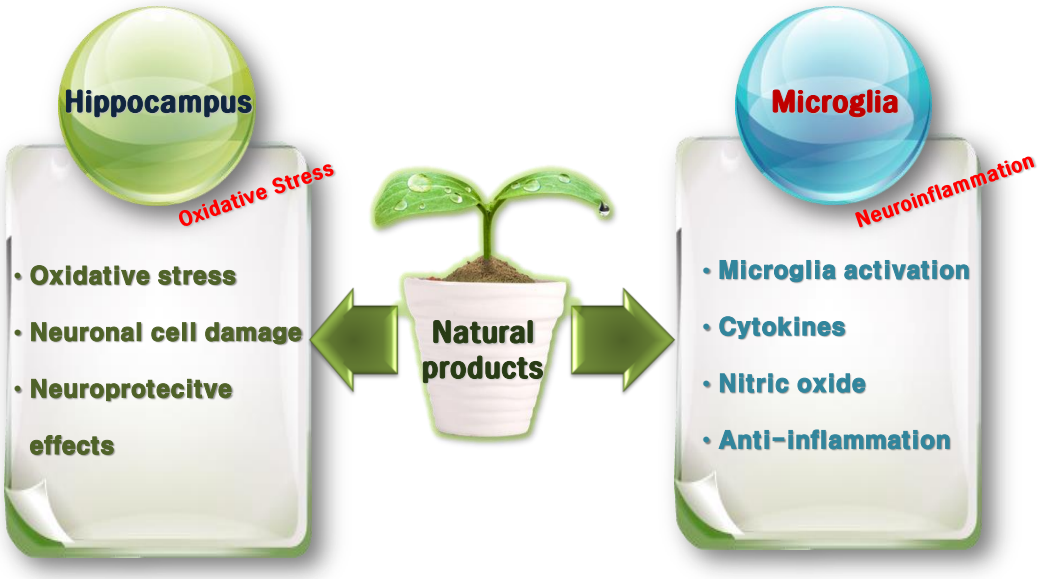

Fig. 3: Cell biological approach using neuronal cell lines

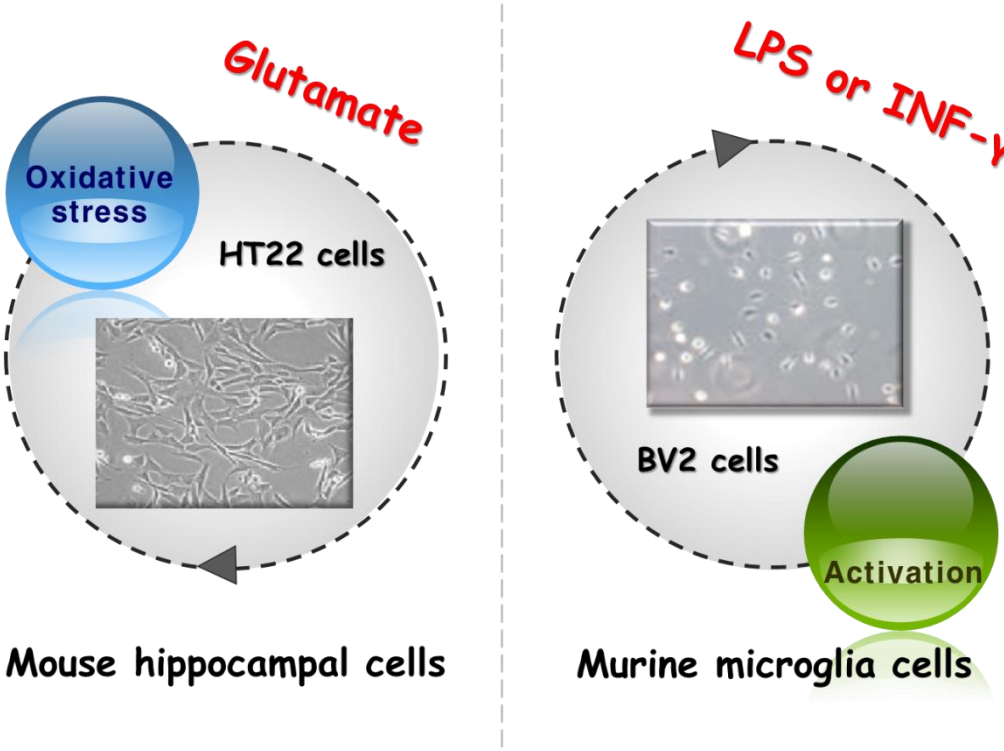

Fig. 4: Mouse hippocampal HT22 cells & murine microglia BV2 cells

2. Materials and Methods

2.1. Materials

2.1.1. Plant Material

The stem of *F. japonica* were collected from Chosun University Herb garden, Gwangju, Korea, in September 2014 and identified by Prof. Eun Rhan Woo, Department of Pharmacy, Chosun University. A voucher specimen has been deposited in the Herbarium of the College of Pharmacy, Chosun University.

2.1.2. Chemicals, reagents and chromatography for isolation

TLC and column chromatography(C.C.) were performed on pre-coated Silica Gel F plates (Merck, art. 5715), RP-18F plates (Merck, art. 15389) and silica gel 60 (40-63 and 63-200 mm, Merck), MCI gel CHP20P (75-150m, Mitsubishi Chemical Co.), Sephadex LH-20 (25-100 μm, Sigma) as well as LiChroprep RP-18 (40-63 μm, Merck) and MPLC (Grace, USA, Reveleris flash Chromatography system, Part No. 5148513). Low pressure liquid chromatography was carried out over a Merck Lichroprep Lobar® -A RP-18 (240 X 9 X 10 mm) column with a FMI QSY-0 pump (ISCO).

2.1.3. Chemicals and reagents for cell culture

Phosphate-buffered saline (PBS) [10 mM phosphate buffer (pH 7.4), 137 mM NaCl, and 2 mM KCl] was purchased from Amresco (Solon, OH). Fetal Bovine Serum (FBS) were purchased from Welgene (Daegu, Korea). All other chemicals were obtained from Sigma (St. Louis, MO) unless otherwise stated.

2.2. Methods

2.2.1. General experimental procedures

Optical rotations were measured using an Autopol-IV polarimeter. IR spectra were recorded on an IMS 85 (Bruker). CD spectra were recorded on a JASCO J-810 spectropolarimeter. HR-ESI–MS spectra were obtained on a Q- TOF (Synapt HDMS system, Waters, USA) mass spectrometer. NMR spectra, COSY, heteronuclear single quantum coherence (HSQC) and HMBC experiments, were recorded on a Varian UNITY INOVA 500 NMR spectrometer (KBSI - Gwangju center) operating at 600 and 500 MHz for both ^{1}H and ^{13}C, with chemical shifts given in ppm (δ). Semi-preparative HPLC was performed using a Waters HPLC system equipped with Waters 600 Q-pumps, Waters 1525 Binary HPLC Pump, a 996 photodiode array detector, a Type-MG column (250×4.6 mm i.d., 5 μm) and an YMC-Pack ODS-A column (250×10 mm i.d., 5 μm), flow rate 4.0 mL/min.

2.2.2. Extraction and Isolation

2.2.2.1. Extraction

The stem of the dry *f. japonica* (5 kg) was cut out and extracted three times with Methanol (MeOH) at 80 ° C for 2 hours. Only some of them were evaporated to gain 252.49 g of MeOH extract. Half of the resulting MeOH extract (112.9 g) was dissolved in water (1.5 L x 3) and partitioned with chloroform ($CHCl_3$), ethyl acetate (EtOAc) and normal-butyl alcohol (n-BuOH). The partitioned fractions were evaporated to give $CHCl_3$ (11.9 g), EtOAc (3.3 g), *n*-BuOH (32.0 g) and an aqueous fraction (50.984 g), respectively (**Scheme 1**).

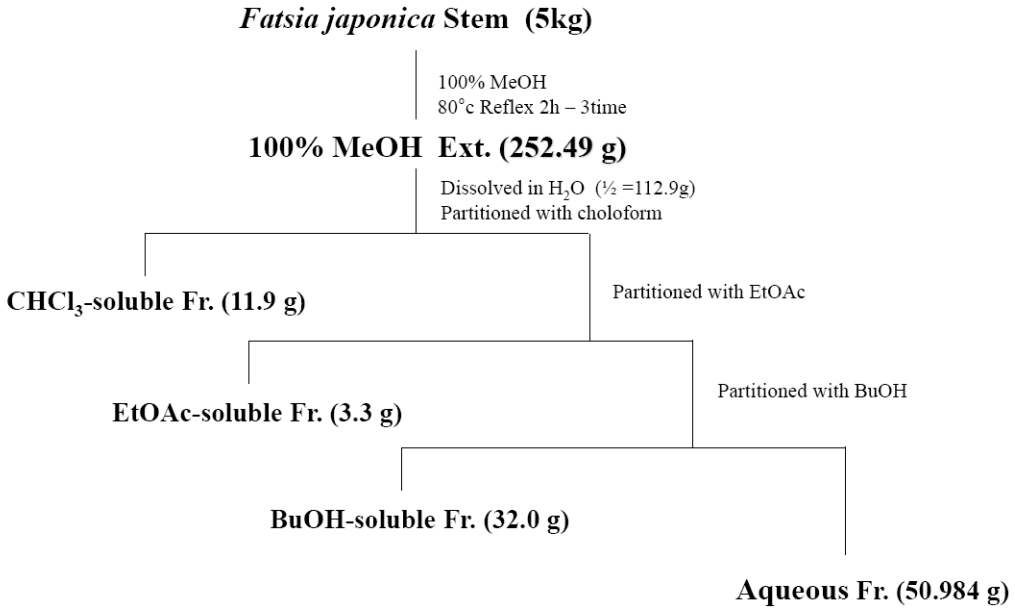

Scheme 1: Extraction and fraction from *Fatsia japonica* Stem

2.2.2.2. Isolation

2.2.2.2.1. Isolation of fraction FJB

The *n*-BuOH fraction (1.0 g) was separated by MPLC using a $CHCl_3$: MeOH: aqueous (5:1:0.1→1:1:0.1) gradient solvent system to gain 10 sub-fractions (FJB1 ~10) (**scheme. 2**).

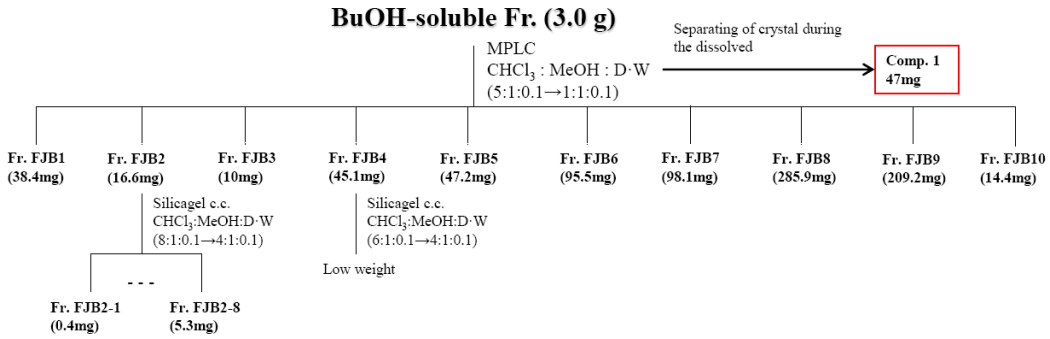

Scheme 2: Isolation of fraction FJB1-10 from *n*-BuOH fraction of *Fatsia japonica* Stem

2.2.2.2.2. Isolation of fraction FJBS

The *n*-BuOH fraction (2.5 g) was separated by MPLC using a $CHCl_3$: MeOH: aqueous (5:1:0.1→1:1:0.1) gradient solvent system to gain 14 sub-fractions (FJBS1 ~14) (**scheme. 3**).

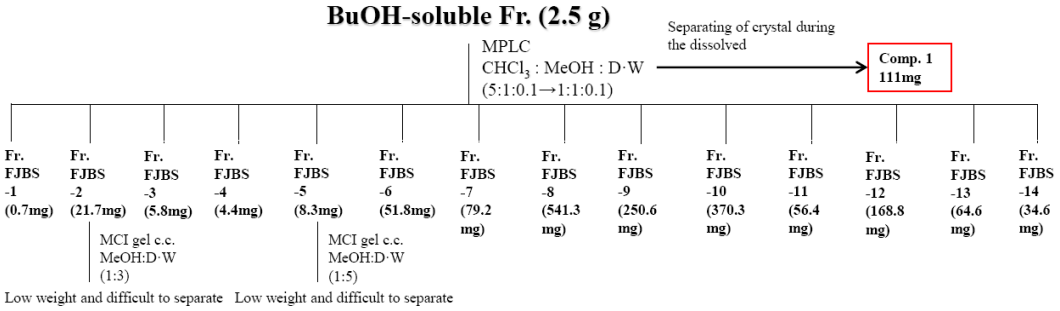

Scheme 3: Isolation of fraction FJBS1-14 from *n*-BuOH fraction of *Fatsia japonica* Stem

2.2.2.2.3. Isolation of fraction FJBH

The *n*-BuOH fractions (7.0g) were separated by HP20 C.C. using MeOH: aqueous (1:0→0:1) gradient solvent system to gain 7 sub-fractions (FJBH1 ~7) (**scheme. 4**).

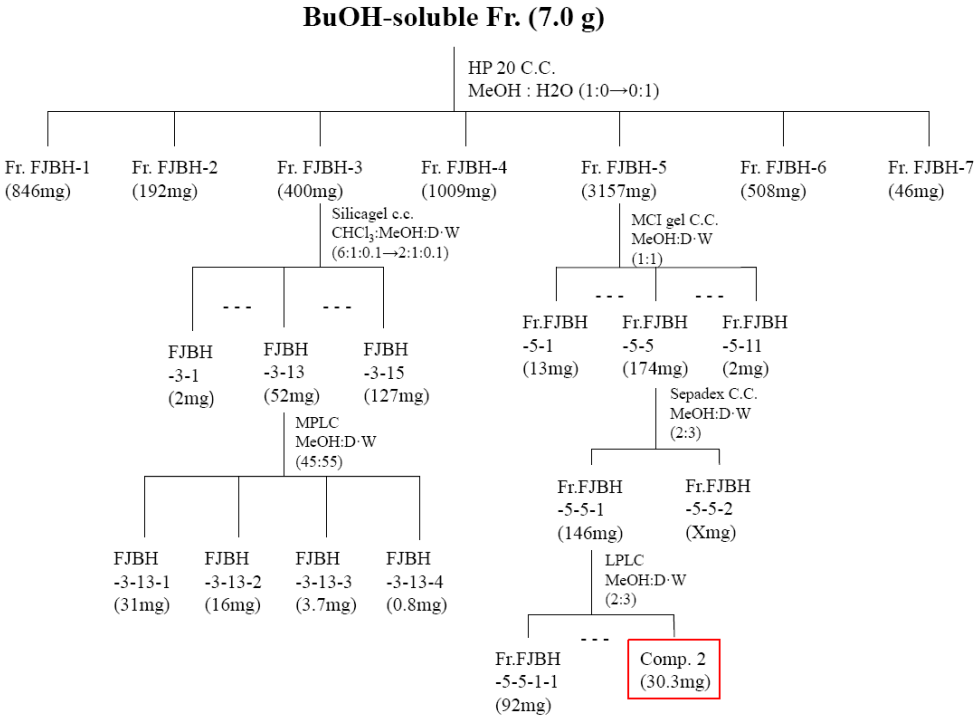

Scheme 4: Isolation of fraction FJBH1-7 from *n*-BuOH fraction of *Fatsia japonica* Stem

2.2.2.2.4. Isolation of fraction FJBN

The *n*-BuOH fractions (10.0g) were separated by silica gel C.C. using a $CHCl_3$: MeOH: aqueous (6:1:0.1→1:1:0.1) gradient solvent system to gain 7 sub-fractions (FJBN1 ~7) (**scheme. 5**).

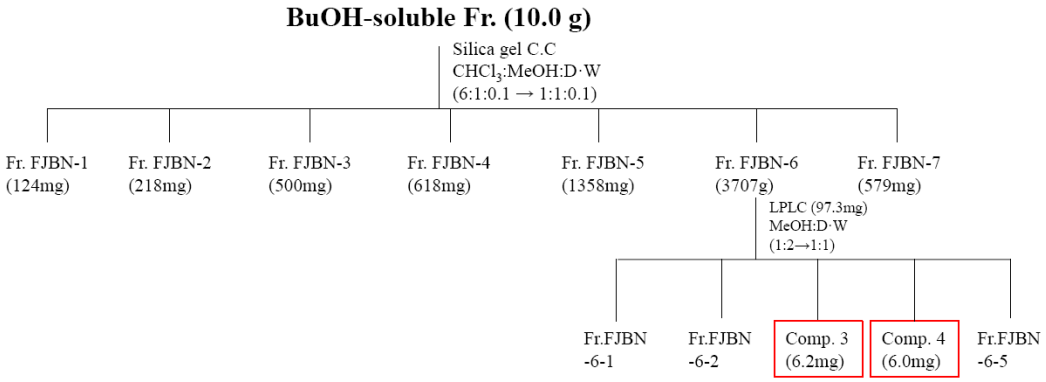

Scheme 5: Isolation of fraction FJBN1-7 from *n*-BuOH fraction of *Fatsia japonica* Stem

2.2.3. Structure identification of compounds

Compound 1:

In the process of dissolving the *n*-BuOH fraction (3.5g) of the *F. japonica* stem in the MeOH solvent, crystals were precipitated, and the precipitated crystals were selected as Compound 1(158mg).

Appearance: Crystal

Molecular formula: $C_{12}H_{22}O_{11}$

Molecular weight: 342.30

Melting point: 102-103℃

$[\alpha]_D^{20}$ = + 130.4 (*c* 0.1, H_2O)

IR (KBr): ν_{max} 3450(OH), 2929, 2850(CH), 1470(OH def.), 1169–1020 (C-O-C), 730–720 cm-1

^{1}H-NMR (500 MHz, DMSO-D_6) δ:

5.17 (1H, J=3.7, H-1), 3.56 (1H, H-2), 3.47 (1H, H-3), 3.88 (H-1, =J9.2, H-4), 3.17 (1H, H-5), 3.58 (1H, H-6a), 3.49 (1H, H-6b), 4.79 (1H, H-1'), 3.65 (1H, H-2'), 3.77 (1H, H-3'), 3.12 (1H, J = 9.3, H-4'), 3.56 (1H, H-5'), 3.40 (2H, J=12.3, H-6').

^{13}C NMR (500 MHz, DMSO-D_6) δ:

91.77 (C-1), 82.57 (C-2), 72.89 (C-3), 77.05 (C-4), 71.65 (C-5), 60.51 (C-6), 104.05 (C-1'), 72.83 (C-2'), 74.31 (C-3'), 69.87 (C-4'), 62.16 (C-5'), 62.08 (C-6').

Compound 2:

The sub-Fraction FJBH-5(3157mg) was separated by MCI gel C.C. using a MeOH: aqueous (1:1) isocratic solvent system to gain 11 sub-fractions (FJBH-5-1~ FJBH-5-11). The 5th fraction (FJBH-5-5, 174mg) of the 11 sub-Fraction from the FJBH-5 fraction was separated by sepadex C.C. using a MeOH: aqueous (2:3) isocratic solvent system to gain 2 fractions (FJBH-5-5-1, 2). The 1st fraction (FJBH-5-5-1, 52mg) of the 2 sub-Fraction from the FJBH-5-5 fraction was separated by LPLC using a MeOH: aqueous (2:3) isocratic solvent system to gain 4 fractions (FJBH-5-5-1-1~ 4), of which fraction FJBH-5-5-1-4 was identified as a single compound and designated as compound 2(30.3mg)

Appearance: white amorphous powder

Molecular formula: $C_{59}H_{96}O_{26}$

Molecular weight: 1221.38

$[\alpha]_D^{25}$ 42.5 (*c* 0.1, MeOH)

HRESIMS: *m/z* 1243.6039 $[M + Na]^+$ (calcd for C59H96O26Na, 1243.6088)

MS/MS (parent ion 1243.6): *m/z* 1097.4 $[M - 146 + Na)]^+$, 935.4 $[M - (146 + 162) + Na)]^+$, 773.4 $[M - (146 + 162 + 162) + Na)]^+$.

^{1}H-NMR (500 MHz, DMSO-D_6) δ:

2.98 (1H, m, H-3), 5.15 (1H, br, s, H-12), 2.73 (1H, dd, J = 4, 14.5, H-18), 1.23 (3H, s, H-23), 0.74 (3H, s, H-24), 0.86 (3H, s, H-25), 0.68 (3H, s, H-26), 0.95 (3H, s, H-27), 0.87 (3H, br, s, H-29), 1.07 (3H, br, s, H-30), Glue-1: 5.20 (1H, d, J = 6 Hz, H-1), Glue-2: 4.69 (1H, br, s, H-1), Glue-3: 4.40 (1H, d, J = 5 Hz, H-1), Ara: 4.33 (1H, d, J = 8 Hz, H-1), Rha: 4.26 (1H, d, J = 8 Hz, H-1), 1.09 (3H, s, H-6).

^{13}C NMR (500 MHz, DMSO-D_6) δ:

38.12 (C-1), 27.27 (C-2), 87.99 (C-3), 39.90 (C-4), 54.98 (C-5), 22.13 (C-6), 32.29 (C-7), 38.73 (C-8), 47.10 (C-9), 36.31 (C-10), 23.40 (C-11), 121.71 (C-12), 143.45 (C-13), 41.33 (C-14), 28.72 (C-15), 22.48 (C-16), 46.00 (C-17), 40.73 (C-18), 45.56 (C-19), 30.32 (C-20), 31.72 (C-21), 33.28 (C-22), 29.03 (C-23), 16.19 (C-24), 15.23 (C-25), 16.72 (C-26), 27.64 (C-27), 175.32 (C-28), 32.77 (C-29), 25.52 (C-30), Glue-1: 94.03 (C-1), 74.54 (C-2), 78.62 (C-3), 71.26 (C-4), 76.54 (C-5), 69.88 (C-6), Glue-2: 100.56 (C-1), 75.23 (C-2), 76.76 (C-3), 69.28 (C-4), 76.45 (C-5), 59.96 (C-6), Glue-3: 103.32 (C-1), 75.51 (C-2), 76.94 (C-3), 67.57 (C-4), 76.39 (C-5), 60.87 (C-6), Ara: 103.82 (C-1), 72.25 (C-2), 71.96 (C-3), 66.36 (C-4), 63.17 (C-5), Rha: 102.57 (C-1), 70.69 (C-2), 70.66 (C-3), 73.79 (C-4), 168.63 (C-5), 17.78 (C-6).

Compound 3:

The sub-Fraction FJBN-6(3707mg) was separated by LPLC using a MeOH: aqueous (1:2→1:1) gradient solvent system to gain 5 sub-fractions (FJBN-6-1~ 5), of which fraction FJBN-6-3 was identified as a single compound and designated as compound 3(6.2mg)

Appearance: white amorphous powder

Molecular formula: $C_{59}H_{96}O_{27}$

Molecular weight: 1237.38

Melting point: 190-195 ℃

$[\alpha]_D^{20}$ = + 42.5 (*c*= 0.81, MeOH)

ESI-MS (pos.): m/z 1225 ($[M + NH_4]^+$), 1238 ($[M + H]^+$), $C_{59}H_{97}O_{27}^+$), 1076 ($[M + H – 162]^+$), 914 ($[M + H – 162 – 162]^+$), 944 ($[M + H – 162 + 132]^+$), 782 ($[M + H – 162 – 162 + 132]^+$), 752 ($[M + H – 162 – 162 – 162]^+$).

ESI-MS (neg.): m/z 1236($[M – H]^-$).

^{1}H-NMR (500 MHz, DMSO-D_6) δ:

2.98 (1H, m, H-3), 5.17 (1H, br, s, H-12), 2.74 (1H, dd, J = 4, 14.5, H-18), 0.74 (3H, s, H-24), 0.86 (.H, s, H-25), 0.68 (3H, s, H-26), 0.95 (3H, s, H-27), 0.87 (3H, s, H-29), 1.07 (3H, s, H-31), Glue-1: 5.20 (1H, d, J = 6 Hz, H-1), Glue-2: 4.69 (1H, br, s, H-1), Glue-3: 4.40 (1H, d, J = 5 Hz, H-1), Ara: 4.33 (1H, d, J = 8 Hz, H-1), Rha: 4.26 (1H, d, J = 7.5 Hz, H-1), 1.09 (3H, s, H-6).

^{13}C NMR (500 MHz, DMSO-D_6) δ:

38.54 (C-1), 27.66 (C-2), 88.39 (C-3), 40.20 (C-4), 55.39 (C-5), 22.91 (C-6), 32.70 (C-7), 39.14 (C-8), 47.51 (C-9), 36.72 (C-10), 23.82 (C-11), 122.12 (C-12), 143.87

(C-13), 41.74 (C-14), 25.98 (C-15), 23.41 (C-16), 46.41 (C-17), 41.14 (C-18), 45.96 (C-19), 30.73 (C-20), 32.14 (C-21), 33.67 (C-22), 62.07 (C-23), 16.61 (C-24), 15.64 (C-25), 17.14 (C-26), 28.05 (C-27), 175.71 (C-28), 33.18 (C-29), 25.93 (C-30), Glue-1: 94.43 (C-1), 74.95 (C-2), 79.03 (C-3), 71.66 (C-4), 76.95 (C-5), 70.28 (C-6), Gluc-2: 100.97 (C-1), 75.64 (C-2), 77.18 (C-3), 69.69 (C-4), 76.84 (C-5), 60.37 (C-6), Gluc-3: 103.72 (C-1), 75.93 (C-2), 77.36 (C-3), 67.97 (C-4), 76.81 (C-5), 61.27 (C-6), Ara: 104.24 (C-1), 72.62 (C-2), 72.37 (C-3), 66.75 (C-4), 63.54 (C-5), Rha: 102.98 (C-1), 71.11 (C-2), 71.07 (C-3), 74.20 (C-4), 69.04 (C-5), 18.20 (C-6).

Compound 4:

The sub-Fraction FJBN-6(3707mg) was separated by LPLC using a MeOH: aqueous (1:2→1:1) gradient solvent system to gain 5 sub-fractions (FJBN-6-1~ 5), of which fraction FJBN-6-4 was identified as a single compound and designated as compound 4(6.0mg)

Appearance: white amorphous powder

Molecular formula: $C_{65}H_{106}O_{32}$

Molecular weight: 1399.52

Melting point: 231-233 ℃

$[\alpha]_D^{20}$ = - 9.57° (c=0.47, MeOH);

FABMS (neg.): m/z: 1397 $[M-H]^-$, 1251 $[M – Rha – H]^-$, 1235 $[M - Glc – H]^-$, 1089 [M - Rha - Glc]-, 927 $[M - Rha - 2Glc – H]^-$, 765 $[M - Rha - 3Glc - H]^-$, 603 [M - Rha - 4Glc - $H]^-$, 471 [M - Rha-4Glc-Ara-$H]^-$.

^{1}H-NMR (500 MHz, DMSO-D_6) δ:

2.98 (1H, m, H-3), 5.17 (1H, br, s, H-12), 2.74 (dd, 1H, J = 4, 14.5Hz, H-18), 0.73 (3H, s, H-24), 0.85 (3H, s, H-25), 0.67 (3H, s, H-26), 0.95 (3H, s, H-27), 0.86 (3H, s, H-29), 1.07 (3H, s, H-30), 2.02 (1H, s, H-32), Rha: 1.09 (3H, s, H-6)

Glue-1: 5.20 (1H, m, H-1), Glue-2: 4.69 (1H, m, H-1), Glue-3: 4.40 (1H, d, J = 5 Hz, H-1), Glue-4: 4.59 (1H, m, H-1) Ara: 4.33 (1H, d, J = 8 Hz, H-1), Rha: 4.29 (1H, d, J = 8 Hz, H-1), 1.09 (3H, s, H-6).

^{13}C NMR (500 MHz, DMSO-D_6) δ:

38.53 (C-1), 27.68 (C-2), 88.39 (C-3), 40.20 (C-4), 55.40 (C-5), 22.92 (C-6), 32.72 (C-7), 39.14 (C-8), 47.52 (C-9), 36.73 (C-10), 23.80 (C-11), 122.13 (C-12), 143.87 (C-13), 41.75 (C-14), 25.99 (C-15), 23.39 (C-16), 46.41 (C-17), 41.15 (C-18), 45.97 (C-19), 30.74 (C-20), 32.11 (C-21), 33.69 (C-22), 63.29 (C-23), 16.61 (C-24),

15.64 (C-25), 17.14 (C-26), 28.06 (C-27), 175.69 (C-28), 33.19 (C-29), 25.94 (C-30), 170.61 (C-32), 21.11 (C-31), Glue-1: 94.42 (C-1), 74.96 (C-2), 79.05 (C-3), 71.66 (C-4), 76.94 (C-5), 70.29 (C-6), Glue-2: 100.97 (C-1), 75.64 (C-2), 77.18 (C-3), 69.70 (C-4), 77.31 (C-5), 60.37 (C-6), Glue-3: 103.73 (C-1), 75.93 (C-2), 77.37 (C-3), 68.18 (C-4), 76.81 (C-5), 61.28 (C-6), Glue-4: 101.36 (C-1), 75.43 (C-2), 77.93 (C-3), 70.99 (C-4), 72.71 (C-5), 69.42 (C-6), Ara: 104.25 (C-1), 72.64 (C-2), 72.25 (C-3), 66.75 (C-4), 63.54 (C-5), Rha: 102.88 (C-1), 71.11 (C-2), 71.08 (C-3), 74.00 (C-4), 69.04 (C-5), 18.17 (C-6).

2.2.4. Cell culture

Mouse hippocampal HT22 cells, murine microglia BV2 cells, and RAW264.7 cells were donated from Prof. Youn-Chul Kim Wonkwang University (Iksan, Korea). The cells (5×10^6/dish) were seeded in 100 mm dishes in DMEM (HT22), alpha-MEME (BV2), or RPMI-1640 (RAW264.7) containing streptomycin (100 μg/mL), 10% heat-inactivated fetal bovine serum (FBS), and penicillin G (100 units/mL), and then incubated at 37 ℃ in a humidified atmosphere (5% CO_2 and 95% air).

2.2.5. MTT assay

To determine cell viability by MTT assay, cells were maintained at 2×10^4 cells/well and then treated with samples in the absence or presence of glutamate (5 mM). After incubation for the indicated times, I removed the cell culture medium from each well, and then replaced with 200 μL of fresh medium in each well. Cells were incubated with 0.5 mg/mL of MTT for 1 h, and the formed formazan were resolved in DMSO.

2.2.6. Nitrite Assay

To determine the NO levels, the concentration of nitrite was assessed by the Griess reaction. The supernatant (100 μL) was mixed with Griess reagent (100 μL), and then determined the absorbance at 525 nm with an ELISA plate reader from BIO-RAD (Hercules, CA, USA).

2.2.7. Western blot analysis

The cells were harvested and pelleted by centrifugation at 200 × g for 3 min.

Then, the cells were washed with PBS and lysed in 20 mM Tris-HCl buffer (pH 7.4) containing a protease inhibitor mixture (0.1 mM phenylmethanesulfonyl fluoride, 5 mg/ml aprotinin, 5 mg/ml pepstatin A, and 1 mg/ml chymostatin). Protein concentration was determined using a Lowry protein assay kit (Sigma Chemical Co.). Thirty microgram of protein from each sample was resolved by 7.5% and 12% sodium dodecyl sulfate-polyacrylamide gel electrophoresis (SDS-PAGE), and then electrophoretically transferred onto a Hybond enhanced chemiluminescence (ECL) nitrocellulose membrane (Bio-Rad, Hercules, CA, USA). The membrane was blocked with 5% skimmed milk and sequentially incubated with the primary antibody (Santa Cruz Biotechnology and Cell Signaling Technology) and a horseradish peroxidase-conjugated secondary antibody followed by ECL detection (Amersham Pharmacia Biotech, Piscataway, NJ, USA).

2.2.8. PGE_2 Assay

The culture medium was collected and the level of PGE2 present in each sample was determined using a commercially available kit from R & D Systems, Inc. The assays were performed according to the manufacturer's instructions.

2.2.9. Statistical Analysis

Data are expressed as the mean ± SD of three independent experiments. Statistical analysis was conducted by GraphPad Prism software version 3.03 from GraphPad Software Inc. (San Diego, CA, USA). The differences between means were assessed by one-way analysis of variance (ANOVA) followed by *Newman-Keuls post hoc test*, and statistical significance was defined at $P < 0.05$.

3. Results and Discussion

3.1. The anti-inflammatory, anti-neuroinflammatory and neuro-protective action by MeOH extracts and its fractions from *Fatsia japonica*.

Characteristics of neurodegenerative diseases are related with nerve cell death and CNS inflammation. Prolonged inflammation can cause a variety of diseases including arthritis, neurodegenerative disorders, inflammatory bowel disease and septic shock syndrome. In addition, enormous inflammatory reactions cause the pathogenesis by interruption of tissue functions. *F. japonica* is grown wild to eastern Asia, including Korea, Japan, and Taiwan. *F. japonica* is known as ornamental plant, and it is also known that pharmacological action through *F. japonica* leaf is effective for asthma, antitussive, expectorant, ache, gout and rheumatism and so on. However, there are rare studies about the anti-inflammatory, anti-neuroinflammatory, and neuro-protective actions of components from *F. japonica*. Therefore, I have initially checked the anti-inflammatory, anti-neuroinflammatory, and neuro-protective actions of MeOH extracts and fractions from *F. japonica*.

3.1.1. The anti-inflammatory effect of MeOH extracts and fractions from *Fatsia japonica* in RAW264.7 cells.

In RAW264.7 cells, I have checked the anti-inflammatory action by methanol extracts and fractions of *F. japonica* on a various concentrations. First, RAW264.7 cells were treated with MeOH extracts from *F. japonica* and then incubated for 24 h with LPS (1 μg/ml). MeOH extracts inhibited nitrite production (Fig. 5) and prostaglandin E2 (PGE_2) production (Fig. 6) in a concentration-dependent manner. In addition, MeOH extracts also suppressed LPS-induced nitric oxide synthase (iNOS) and cyclooxygenase-2 (COX-2) expression (Fig. 7).

Continually, I also checked the nitrite production of 4 fractions (choloform, ethyl acetate, *n*-buthanol, and water-soluble fraction) of *F. japonica* in RAW264.7 cells. The nitrite production by LPS significantly reduced by choloform, ethyl acetate, and *n*-buthanol-soluble fraction in a concentration dependent manner, but water-soluble fraction did not show any reduction of nitrite production in RAW264.7 cells (Fig. 8). In this experiment, butein isolated from *Rhus verniciflua* was used as a positive control to compare the nitrite inhibitory action.

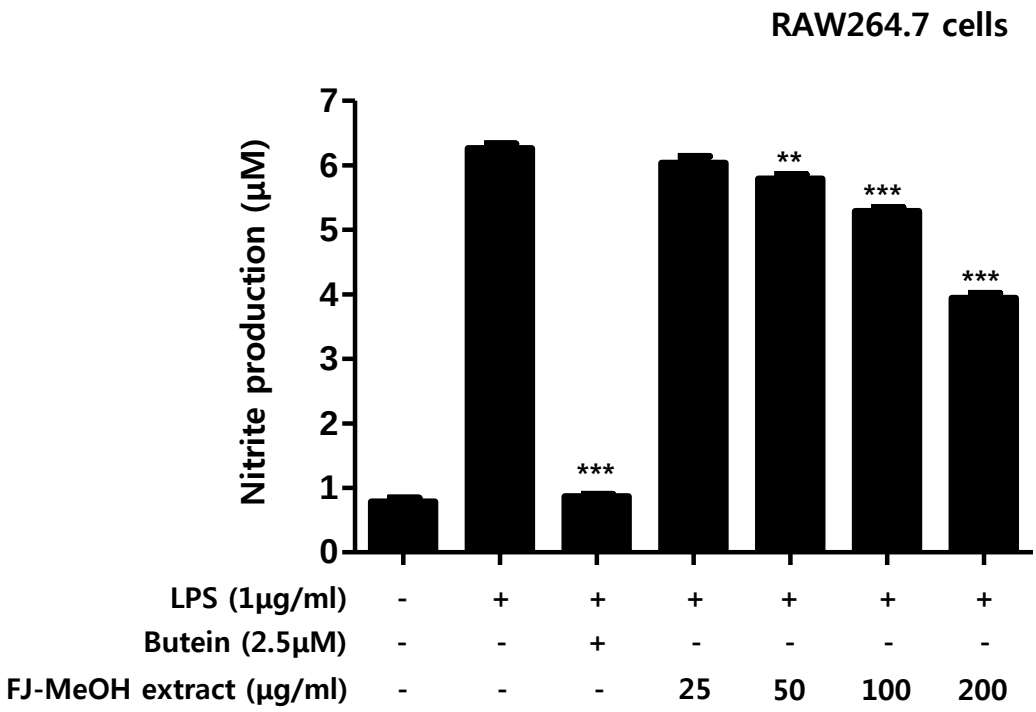

Fig. 5: The effect of MeOH extracts from *Fatsia japonica* on nitrite reduction in RAW264.7 cells. RAW264.7 cells were treated with MeOH extracts from *F. japonica* and then incubated for 24 h with LPS (1 μg/ml). Data are presented as mean ± SD values of 3 independent experiments. Butein (2.5 μM) was used as the positive control. $^{**}P < 0.01$, $^{***}P < 0.001$ vs. LPS.

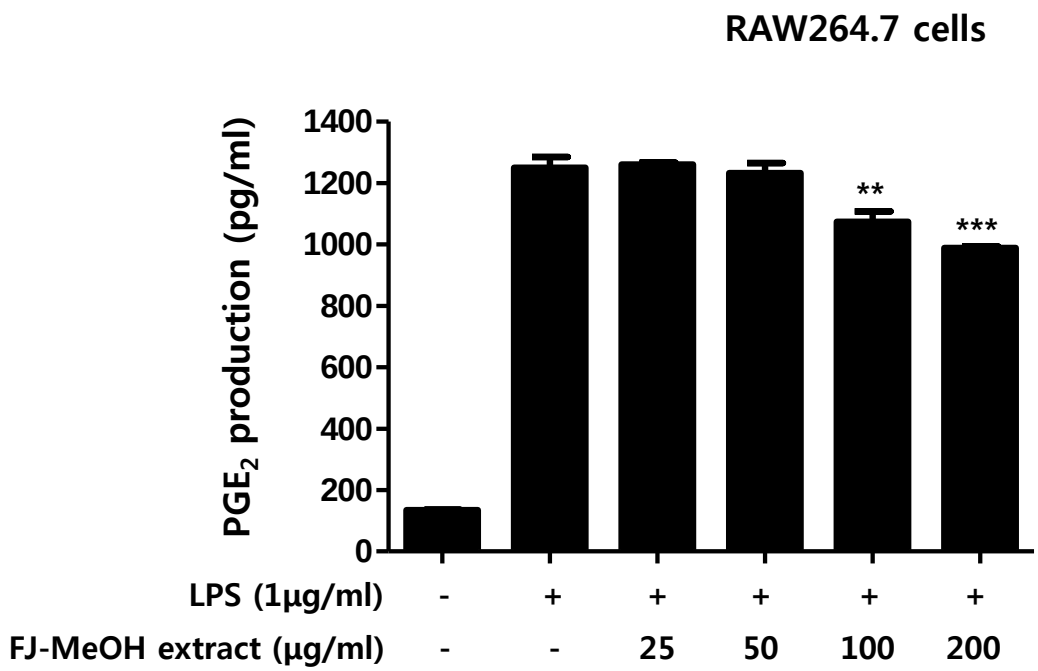

Fig. 6: The effect of MeOH extracts from *Fatsia japonica* on prostaglandin E2 (PGE_2) reduction in RAW264.7 cells. RAW264.7 cells were treated with MeOH extracts from *F. japonica* and then incubated for 24 h with LPS (1 μg/ml). Data are presented as mean ± SD values of 3 independent experiments. $^{**}P < 0.01$, $^{***}P < 0.001$ vs. LPS.

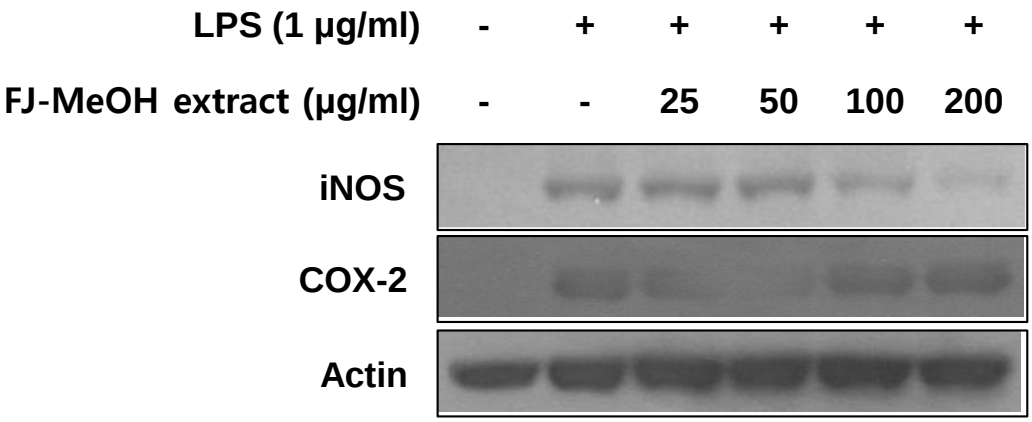

Fig. 7: The effects of MeOH extracts from *Fatsia japonica* on inducible nitric oxide synthase (iNOS) and cyclooxygenase-2 (COX-2) expression in RAW264.7 cells. RAW264.7 cells were treated with MeOH extracts from *F. japonica* and then incubated for 24 h with LPS (1 μg/ml).

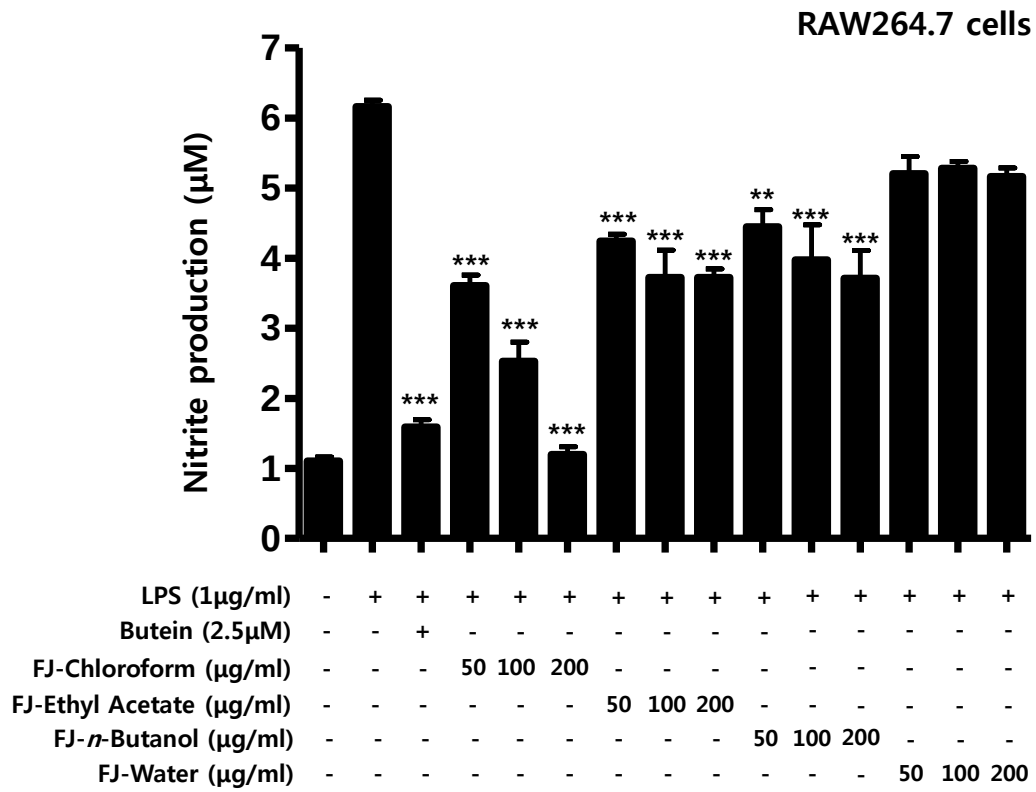

Fig. 8: The effects of fractions from *Fatsia japonica* on nitrite reduction in RAW264.7 cells. RAW264.7 cells were treated with fractions from *F. japonica* and then incubated for 24 h with LPS (1 μg/ml). Data are presented as mean ± SD values of 3 independent experiments. Butein (2.5 μM) was used as the positive control. $^{**}P < 0.01$, $^{***}P < 0.001$ vs. LPS.

3.1.2. The anti-neuroinflammatory effect of MeOH extracts and fractions from *Fatsia japonica* in BV2 cells.

I have also checked the anti-neuroinflammatory action of MeOH extracts and fractions from *F. japonica* in BV2 cells on a various concentrations. First, BV2 cells were treated with MeOH extracts from *F. japonica* and then incubated for 24 h with LPS (1 μg/ml). MeOH extracts inhibited nitrite production (Fig. 9) and prostaglandin E2 (PGE_2) production (Fig. 10) in a concentration-dependent manner. In addition, MeOH extracts also suppressed LPS-induced nitric oxide synthase (iNOS) and cyclooxygenase-2 (COX-2) expression (Fig. 11).

Continually, I have also checked the nitrite production of 4 fractions (choloform, ethyl acetate, *n*-buthanol, and water-soluble fraction) of *F. japonica* in BV2 cells. The nitrite production by LPS significantly reduced by choloform, ethyl acetate, and *n*-buthanol-soluble fraction in a concentration dependent manner, but water-soluble fraction did not show any reduction of nitrite production in BV2 cells (Fig. 12). In this experiment, butein isolated from *Rhus verniciflua* was used as a positive control to compare the nitrite inhibitory action.

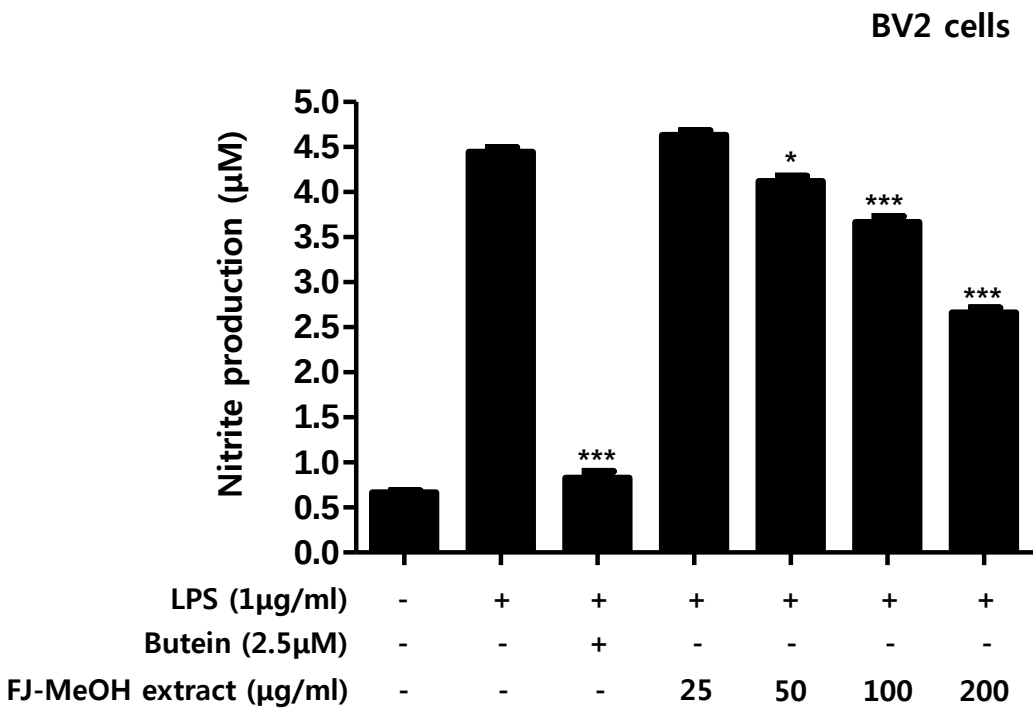

Fig. 9: The effects of MeOH extracts from *Fatsia japonica* on nitrite reduction in BV2 cells. BV2 cells were treated with MeOH extracts from *F. japonica* and then incubated for 24 h with LPS (1 μg/ml). Data are presented as mean ± SD values of 3 independent experiments. Butein (2.5 μM) was used as the positive control. $^{*}P < 0.05$, $^{***}P < 0.001$ vs. LPS.

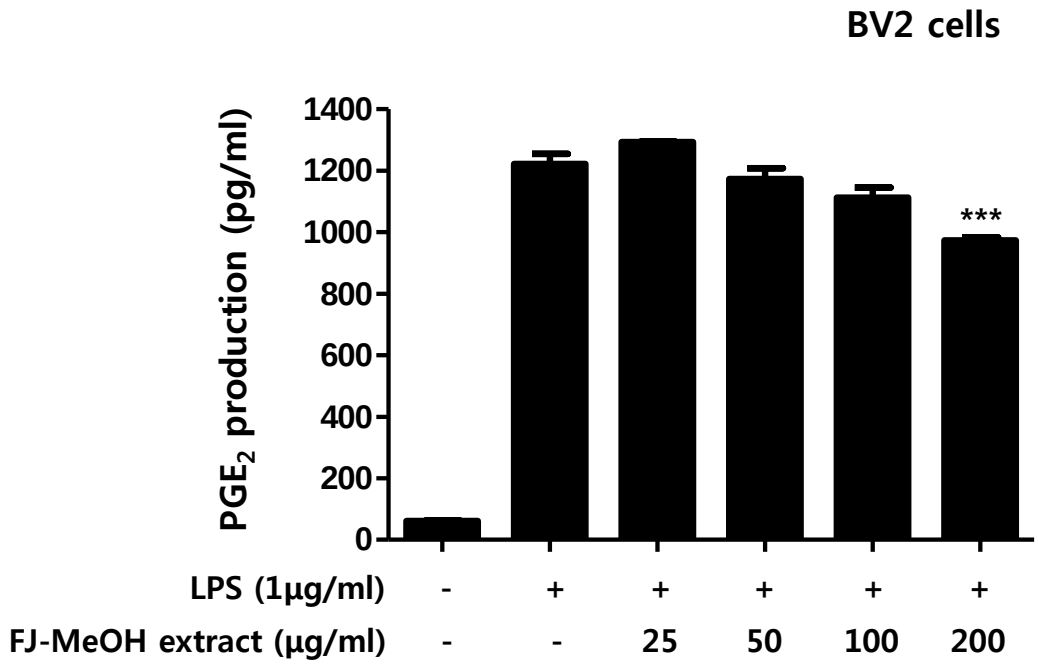

Fig. 10: The effects of MeOH extracts from *Fatsia japonica* on prostaglandin E2 (PGE_2) reduction in BV2 cells. BV2 cells were treated with MeOH extracts from *F. japonica* and then incubated for 24 h with LPS (1 μg/ml). Data are presented as mean ± SD values of 3 independent experiments. $^{***}P < 0.001$ vs. LPS.

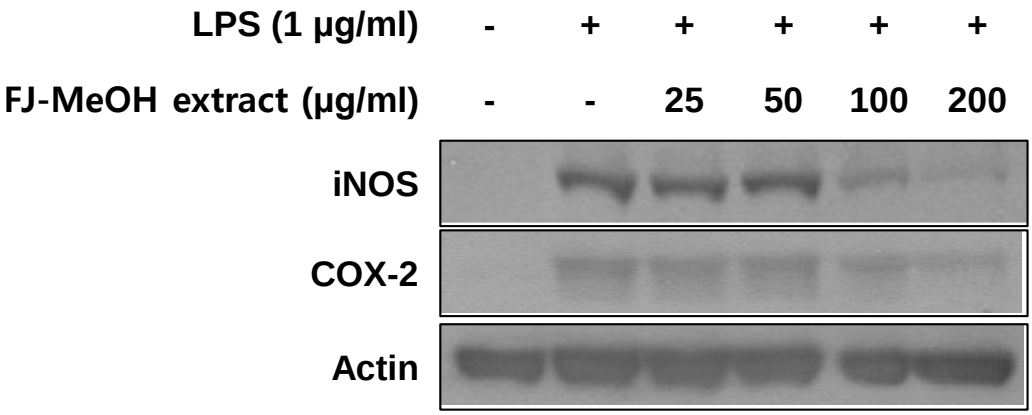

Fig. 11: The effects of MeOH extracts from *Fatsia japonica* on inducible nitric oxide synthase (iNOS) and cyclooxygenase-2 (COX-2) expression in BV2 cells. BV2 cells were treated with MeOH extracts from *F. japonica* and then incubated for 24 h with LPS (1 μg/ml).

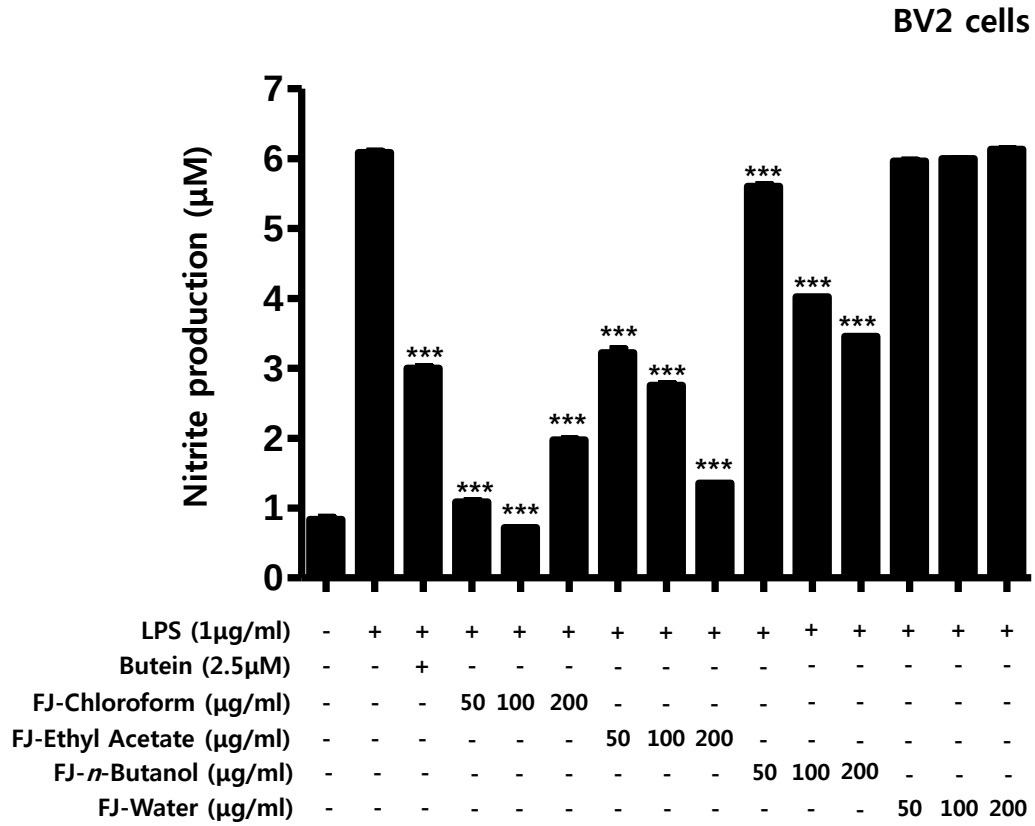

Fig. 12: The effects of fractions from *Fatsia japonica* on nitrite reduction in BV2 cells. BV2 cells were treated with fractions from *F. japonica* and then incubated for 24 h with LPS (1 μg/ml). Data are presented as mean ± SD values of 3 independent experiments. Butein (2.5 μM) was used as the positive control. $^{***}P < 0.001$ vs. LPS.

3.1.3. The neuroprotective effects of MeOH extracts and fractions from *Fatsia japonica* on cell viability by MTT assay in HT22 cells.

Next, I have also checked the neuroprotective action of MeOH extracts and fractions from *F. japonica* in HT22 cells. In HT22 cells, I have checked the neuroprotective action by methanol extracts and fractions of *F. japonica* on a various concentrations. First, HT22 cells were treated with MeOH extracts from *F. japonica* and then incubated for 12 h with glutamate (6.6 mM). MeOH extracts increased cell viability against glutamate-stimulated HT22 cells death (Fig. 13).

Continually, I have also checked the cell protection by 4 fractions (choloform, ethyl acetate, *n*-buthanol, and water-soluble fraction) of *F. japonica* in HT22 cells. The choloform, ethyl acetate, and *n*-buthanol-soluble fraction significantly reduced the glutamate-mediated cell death, but water-soluble fraction did not show any effects in HT22 cells (Fig. 14). In this experiment, butein isolated from *Rhus verniciflua* was used as a positive control to compare the cytoprotective effects.

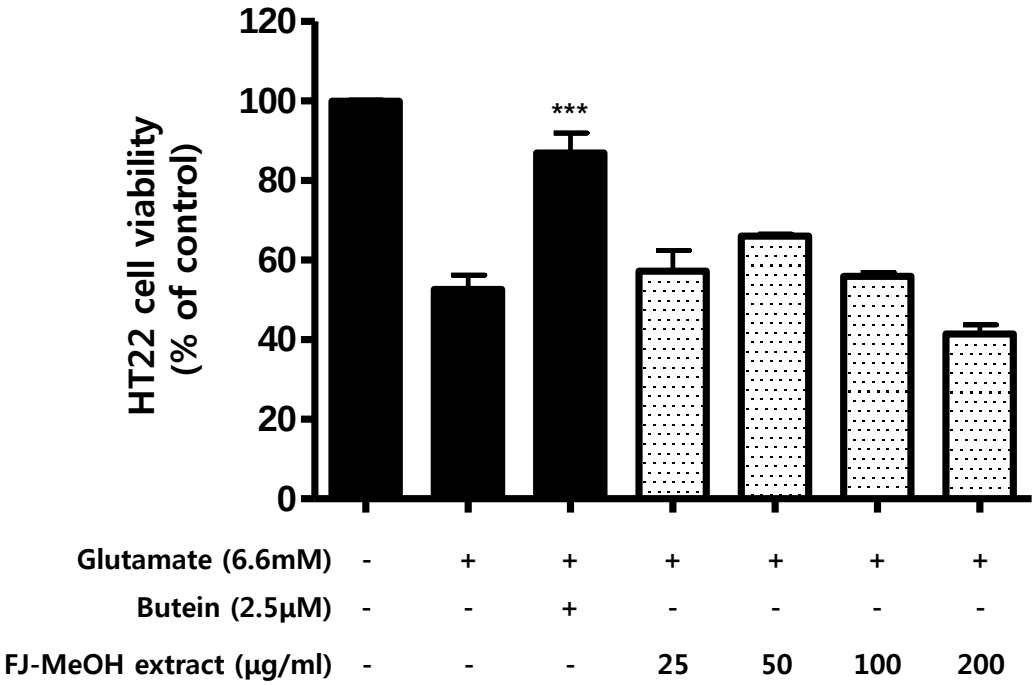

Fig. 13: The effects of MeOH extracts from *Fatsia japonica* on cell viability by MTT assay in HT22 cells. HT22 cells were treated with MeOH extracts from *F. japonica* and then incubated for 12 h with glutamate (6.6 mM). Data are presented as mean ± SD values of 3 independent experiments. Butein (2.5 μM) was used as the positive control. $^{***}P < 0.001$ vs. glutamate.

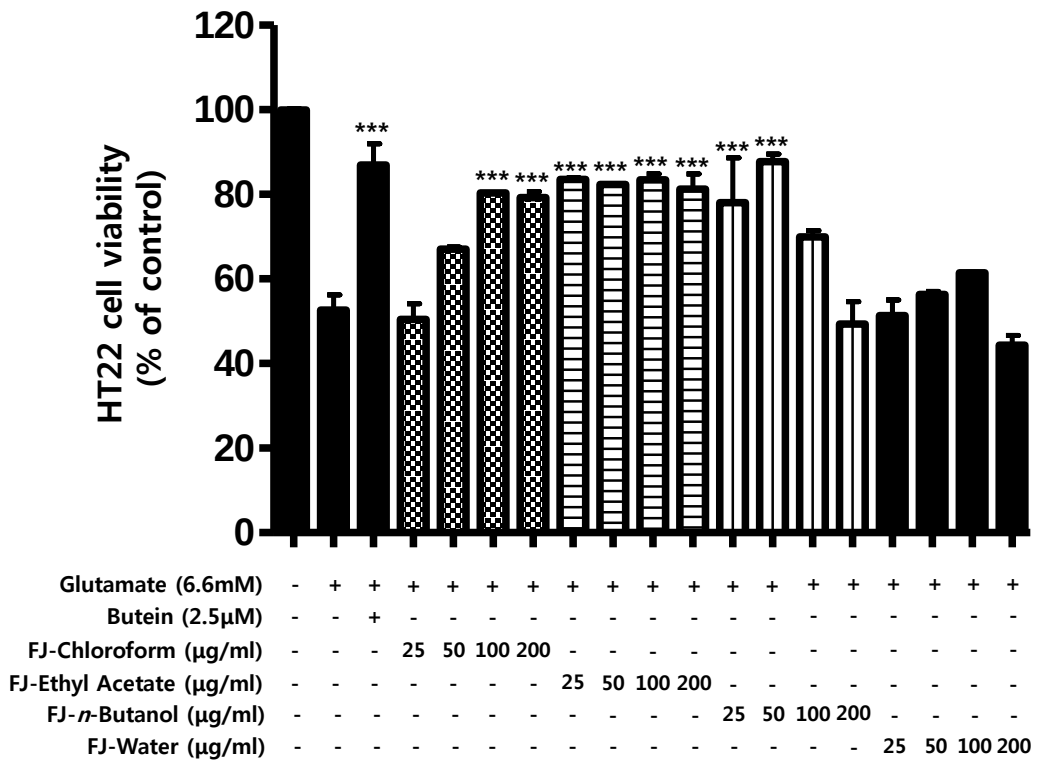

Fig. 14: The effects of fractions from *Fatsia japonica* on cell viability by MTT assay in HT22 cells. HT22 cells were treated with fractions from *Fatsia japonica* and then incubated for 12 h with glutamate (6.6 mM). Data are presented as mean ± SD values of 3 independent experiments. Butein (2.5 μM) was used as the positive control. $^{***}P < 0.001$ vs. glutamate.

3.2. Structure determination of isolated compounds from *Fatsia japonica*.

The structures of compounds (1- 4) were identified based on 1D and 2D NMR, including H - H COSY, HSQC, HMBC spectroscopic analyses.

3.2.1. Compound 1

The assignment of the resonances in maltose was obtained from 1D and 2D NMR, 2D-HSQC, HMBC, DQF-COSY, TOCSY, ROESY and NOESY experiments. From 1H NMR observed 13 hydroxyl proton at δ 5.17 (1H, J=3.7, H-1), 3.56 (1H, H-2), 3.47 (1H, H-3), 3.88 (H-1, =J9.2, H-4), 3.17 (1H, H-5), 3.58 (1H, H-6a), 3.49 (1H, H-6b), 4.79 (1H, H-1'), 3.65 (1H, H-2'), 3.77 (1H, H-3'), 3.12 (1H, J = 9.3, H-4'), 3.56 (1H, H-5'), 3.40 (2H, J=12.3, H-6'). The anomeric carbon at δ 91.77 (C-1) and 104.05 (C-1') indicated the presence of two sugar, which also exhibits two primary alcoholic group at δ 60.51 (C-6) a62.08 (C-6'). From the referred DQF-COSY, TOCSY, ROESY and NOESY data we confirmed the compound 1 identified as Maltose. According to reference, two peaks should be observed for all the CH and OH protons on the reducing residue and for all the protons on the nonreducing residues due to the two anomeric forms of the reducing rings. However, because the anomeric configuration has usually a negligible influence on the conformation, the proton chemical shifts of the nonreducing units are very similar. Thus, 12 hydroxy proton signals were expected for maltose. The NMR spectra revealed the presence of 13 hydroxy proton signals. The DQF-COSY shows the existence of two O(2′)H signals separated by 0.047 ppm giving a COSY cross-peak to two C(2′)H signals separated by 0.005 ppm. In the ROESY spectra, an exchange crosspeak was observed between the O(3)H signal of the reducing β-D-glucose and the signal at δ 6.412 ppm, allowing this signal to be assigned to O(2′)H of β-

maltose [O(2′)H(*β*)]. The signal at *δ* 6.365 ppm was subsequently assigned to the O(2′)H of the sugar linked to the reducing α-D-glucose [O(2′)H(α)]. The corresponding ROE crosspeak was not observed for the α-anomer. The O(2″)H of the sugar at the terminal nonreducing end has a chemical shift of *δ* 6.376 ppm, very similar to the shift measured for O(2′)Hα in maltose (*δ* 6.365 ppm). The O(2′)H of the residue 1,4- linked to the reducing end has a shift of *δ* 6.405 ppm, very similar to the shift measured for O(2′)H(*β*) in maltose (*δ* 6.412 ppm). The O(2′)H of the sugar 1,4-linked to the α-reducing form was not visible in the NMR spectra [30-32].

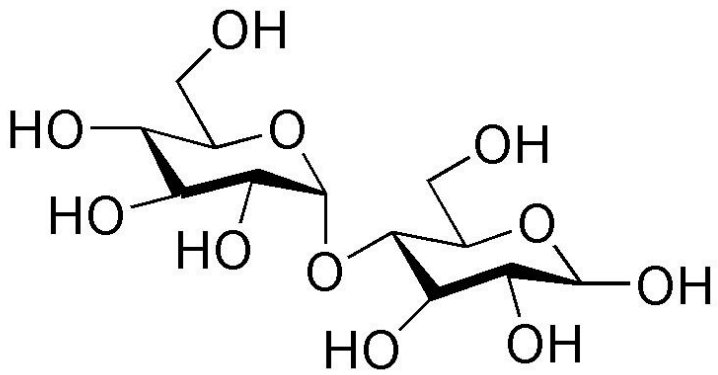

Fig. 15: Structure of compound 1 from *n*-BuOH fraction of *F. japonica.*

3.2.2. Compound 2

Compound 2, named begoniifolide A, and obtained as a white powder, which was considered to be a triterpenoid glycoside. Its molecular formula was determined as $C_{59}H_{96}O_{26}$ according to the negative HRESIMS.

After acid hydrolysis and derivatization of 2, the GC analysis revealed the presence of D-glucose, L-rhamnose and L-arabinose in an approximate ratio of 3:1:1. The ^{1}H NMR spectrum of 2 showed signals for seven tertiary methyl groups at δ 1.23, 0.74, 0.86, 0.68, 0.95, 0.87, and 1.07, five anomeric sugar protons at δ 5.20 (1H, d, J 6 Hz), 4.69 (1H, br, s), 4.40 (1H, d, J 5 Hz), 4.33 (1H, d, J 8 Hz) and 4.26 (1H, d, J 8 Hz), and a series of overlapped signals suggesting an oleanane type triterpene glycoside. A further feature of the ^{1}H NMR spectrum was the signal at δ 5.15 (1H, br. s) typical of H-12, which was also indicated by the signals at δ 121.71 and 143.45 due to C-12 and C-13 in the ^{13}C NMR spectrum. All these data pointed to 3β-12-en-28-oic acid (skeleton).

The comparison of the ^{13}C NMR data of 2 to those of the moieties of the ether-linkage and ester-linkage sugar chains. This deduction was confirmed by the HMBC experiment. The HMBC correlation signals found at δ 4.33 (1H, d, J 8 Hz, Ara, H-1)/87.99(C-3) and 4.40 (1H, d, J 5 Hz, Gluc-3, H-1)/71.96(Ara, C-3) indicated that the ether-linkage sugar chain at C-3 was β-D-glucopyranosyl-(1→3)-α-L-arabinopyranosyl. The HMBC correlation signals found at δ 5.20 (1H, d, J 6 Hz, Gluc-1, H-1)/175.32 (C-28), 4.69 (1H, br, s, Gluc-2, H-1)/69.88 (Gluc-1, C-6) and 4.26 (1H, d. J 8 Hz, Rham, H-1)/69.28 (Gluc-2, C-4) indicated that the ester-linkage sugar chain at C-28 was α-L-rhamnopyranosyl-(1→4)-β-D-glucopyranosyl-(1→6)-β-D-glucopyranosyl. On the basis of these data, 3 was elucidated as 3-O-β-D-glucopyranosyl-(1→3)-α-L-arabinopyranosyl-olean-12-en-28-O-α-L-rhamnopyranosyl-(1→4)-β-D-glucopyranosyl-(1→6)-β-D-glucopyranosyl ester or Begoniifolide A [33, 34].

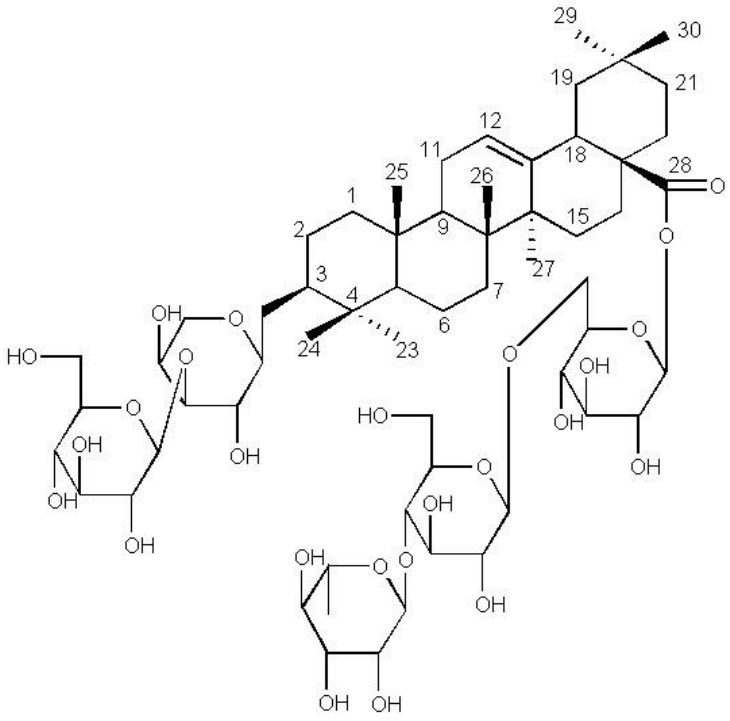

Fig. 16: Structure of compound 2 from *n*-BuOH fraction of *F. japonica*.

3.2.3. Compound 3

Compound 3, named leiyemudanoside B, obtained as a white amorphous powder, which was considered to be a triterpenoid glycoside. Its molecular formula was determined as $C_{59}H_{96}O_{27}$ according to the negative HRESIMS.

After acid hydrolysis of 3, the signals for the aglycone moiety of 3 showed the sugar part derivatization and, the Gas chromatography (GC) analysis revealed the presence of D-glucose, L-rhamnose and L-arabinose in an approximate ratio of 3:1:1. The ^{1}H NMR spectrum of 4 showed signals for six tertiary methyl groups at δ 0.74, 0.86, 0.68, 0.95, 0.87, and 1.07. The presence of five sugars in 3 was apparent from the five anomeric proton signals at δ 5.20(1H, d, J 6 Hz), 4.69 (1H, br, s), 4.40 (1H, d, J 5 Hz), 4.33 (1H, d, J 8.0 Hz) and 4.26(1H, d, J 7.5 Hz), which correlated with the corresponding carbon signals at δ 94.43, 100.97, 103.72, 104.24 and 102.98, respectively, in the HSQC experiment. According to the anomeric protoncoupling constants, the relative configurations of arabinopyranosyl, rhamnopyranosyl and glucopyranosyl units were determined as α, α and β, respectively.

A further feature of the ^{1}H NMR spectrum was the signal at δ 5.17 (1H, br. s) typical of H-12, which was also indicated by the signals at δ 122.12 and 143.87 due to C-12 and C-13 in the ^{13}C NMR spectrum an two oxygenated carbon at δ 62.07 (C-23) and 88.39 (C-3). All these data pointed to 3β-23 hydroxy-12-en-28-oic acid (skeleton). In the HMBC experiment, H-23 showed long-range correlation with C-3, C-4, C-5 and C-24 and thus structural unit could be proposed. The comparison of the ^{13}C NMR data of 4 to those of the moieties of the ether-linkage and ester-linkage sugar chains. This deduction was confirmed by the HMBC experiment. The HMBC correlation signals found at δ 4.33 (1H, d, J 8 Hz, Ara, H-1)/88.39(C-3) and 4.40 (1H, d, J 5 Hz, Gluc-3, H-1)/72.37 (Ara, C-3) indicated that the ether-linkage sugar chain at C-3 was β-D-glucopyranosyl-(1→3)-α-L-arabinopyranosyl. The

HMBC correlation signals found at δ 5.20 (1H, d, J 6 Hz, Gluc-1, H-1)/175.71 (C-28), 4.69 (1H, br, s, Gluc-2, H-1)/70.28 (Gluc-1, C-6) and 4.26 (1H, d. J 7.5 Hz, Rham, H-1)/69.69 (Gluc-2, C-4) indicated that the ester-linkage sugar chain at C-28 was α-L-rhamnopyranosyl-(1→4)-β-D-glucopyranosyl-(1→6)-β-D-glucopyranosyl. On the basis of these data, 3 was elucidated as 3β- [(O-β-D-glucopyranosyl-(1→3)-α-L-arabinopyranosyl)oxy]- 23-hydroxyolean-12-en-28-oic acid O-α-L-rhamnopyranosyl- (1→4)-O-β-D-glucopyranosyl-(1→6)-β-D-glucopyranosyl ester or leiyemudanoside B [34, 35].

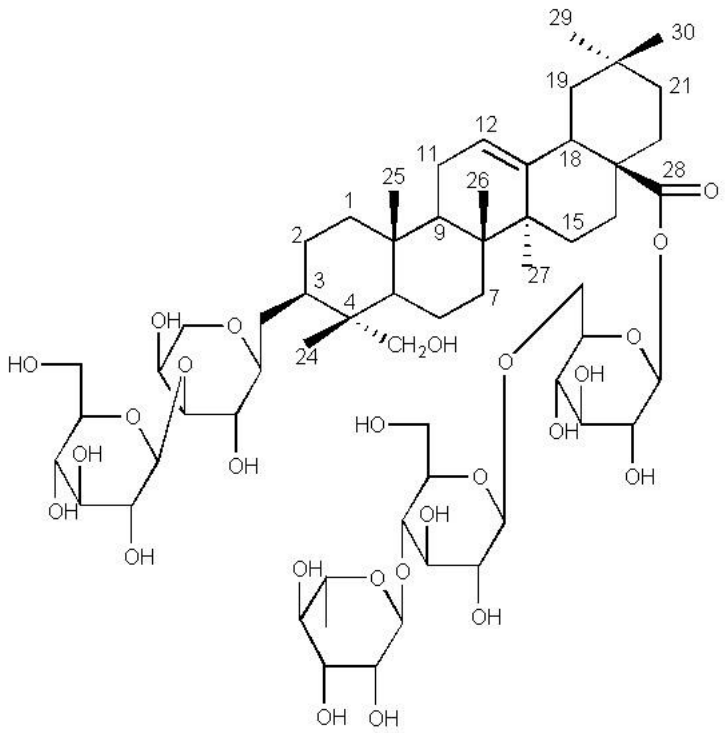

Fig. 17: Structure of compound 3 from *n*-BuOH fraction of *F. japonica*.

3.2.4. Compound 4

The ^{13}C NMR and HSQC data **compound 4** showed 65 carbon and expected triterpenoid typed compound. From the ^{1}H-NMR data **compound 4** showed seven methyl group at δ_H 0.73 (3H, s, H-24), δ_H 0.85 (3H, s, H-25), δ_H 0.67 (3H, s, H-26), δ_H 0.95 (3H, s, H-27), δ_H 0.86 (3H, s, H-29), δ_H 1.07 (3H, s, H-30), and sugar methyl at δ_H 1.09 (3H, s, Rha-H-6). The spectra also exhibited signals due to the following groups at positions similar to those of hederagenin: a carboxylic acid group δ 175.69 (C-28), a trisubstituted double bond δ 122.13 (C-12) and 143.87 (C-13), a proton signal at δ 5.17 (1H, br, s, H-12), a primary alcoholic group δ 63.29 (C-23) and a secondary alcoholic hydroxyl group δ 88.39 (C-3), proton signal at δ 2.98 (1H, m, H-3).

The characterization of the sugar moieties in **compound 4** was accomplished by the analysis of the NMR data obtained from DQF-COSY, TOCSY, T-ROESY, HSQCand HMBC spectra. The spin systems corresponding to the six monosaccharides were clearly discernible in the TOCSY spectrum, walking along pivotal anomeric proton resonances. The complementary data from the DQF-COSY spectrum was used to obtain a full assignment of the proton resonances and to characterize the relative stereochemistry of each of the sugar residues in 4 as β-D-glucopyranose, α-L-rhamnopyranose and α-L-arabinopyranose, respectively. The sequential assignments of the sugar moieties were derived from a cross-relaxation measurement (T-ROESY) and further verified by the HMBC experiment. The arabinose showed ROE_S with H-3 of the aglycone as well as with two terminal glucose residues, indicating the branched nature of the trisaccharide connected at C-3 of the aglycone. Furthermore, the intra-residue ROE correlations arising from the 1,3-diaxial interaction between the anomeric proton and H-3 in glucose residues discriminated the resonances of the glucose H-3 and H-4 protons, which overlapped in the DQFCOSY and TOCSY spectra. Thus, the structure of 4 was

identified as 3-*O*-[*β*-D-glucopyranosyl-(1→3)] - [*β*-D-glucopyranosyl-(1→2)] - *α*-L-arabinopyranosyl - hederagenin 28-0-*α*-L-rhamnopyranosyl - (l→4)-*β*-D-glucopyranosyl-(1→6)-*β*-D-glucopyranoside or leonticin F [36].

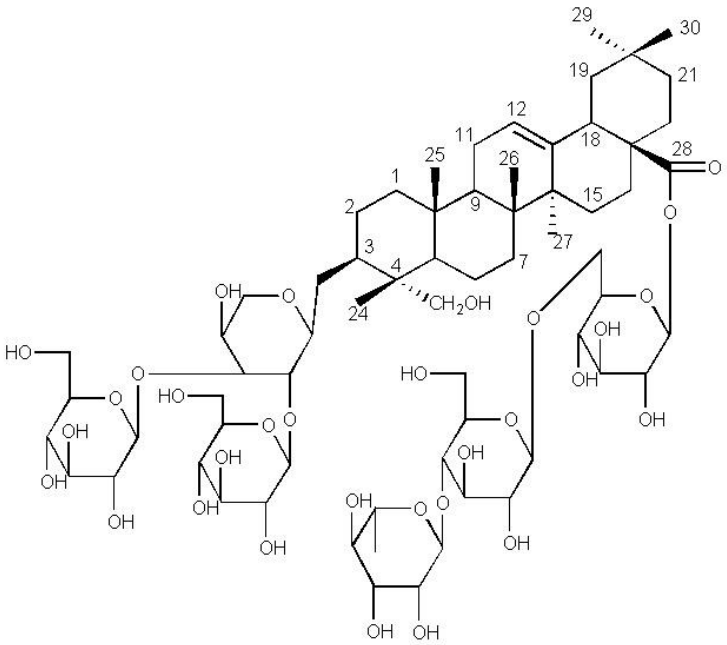

Fig. 18: Structure of compound 4 from *n*-BuOH fraction of *F. japonica*.

3.3. The anti-inflammatory, anti-neuroinflammatory and neuro-protective action by compounds 1-4 from *Fatsia japonica*

Glutamate is the important excitatory neurotransmitter and plays key roles in brain development and processes related to the movement control, memory, and learning in the CNS. However, the overstimulation of glutamate receptors has been involved in the neuronal damage observed in many neurodegenerative diseases. The neuronal HT22 cell line originated from the mouse hippocampus lacks glutamate receptors, therefore it can cause for glutamate mediated cell death. And, microglial cells function as the immune cells of the CNS, acting as primary mediators of inflammation. In response to some negative stimulus such as a free radicals and tissue or organ damages, microglial cells presume a reactive state characterized by the widening and shortening of microglial processes. Activated microglia can produce glutamate transporters and antioxidants to promote correct neuronal function. However, activated microglia is also able to generate several neurotoxic compounds including NO and several pro-inflammatory cytokines that are associated with neurological diseases and CNS disturbances. In CNS inflammation, microglial responses and activation can be mediated from various agents, including LPS and several pro-inflammatory cytokines. Therefore, I have checked the anti-inflammatory, anti-neuroinflammatory, and neuro-protective actions of compounds **1-4** from *F. japonica*. However, there were no effects of compounds **1-4;** maltose (**1**), begoniifolide A (**2**), leiyemudanoside B (**3**), leonticin F (**4**) on the anti-inflammatory, anti-neuroinflammatory, and neuro-protective action.

3.3.1. The effect of compounds 1-4 from *Fatsia japonica* on cell viability and nitrite reduction in RAW264.7 cells.

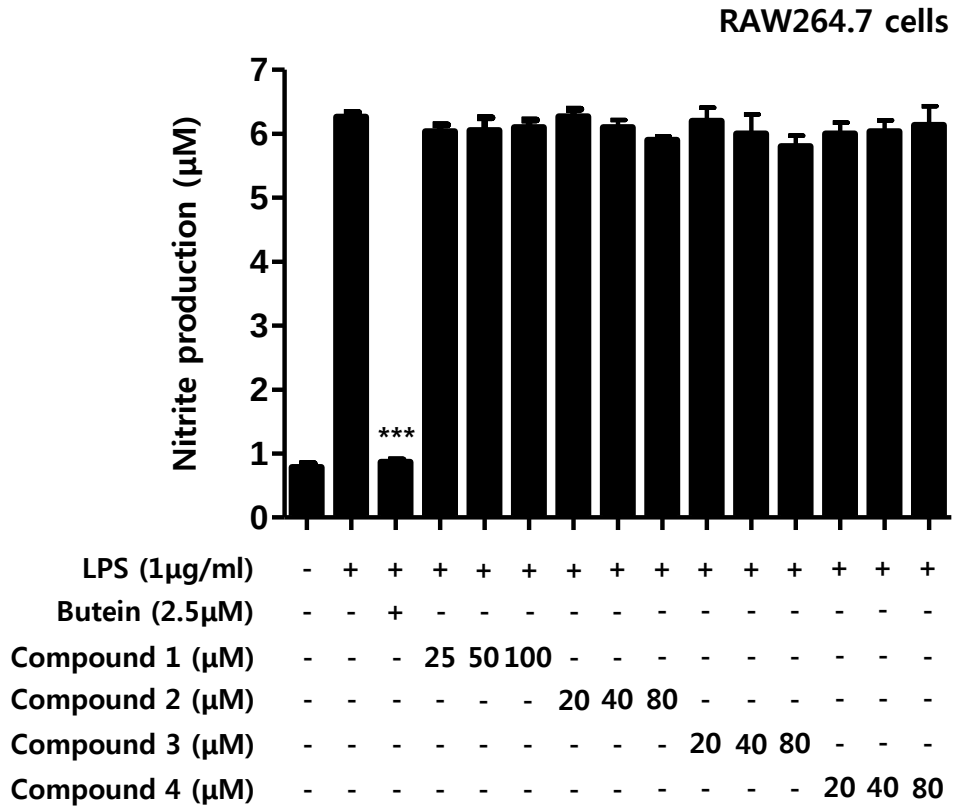

Fig. 19. The effects of compounds 1-4 from *Fatsia japonica* on nitrite reduction in RAW264.7 cells. RAW264.7 cells were treated with fractions from *Fatsia japonica* and then incubated for 24 h with LPS (1 μg/ml). Data are presented as mean ± SD values of 3 independent experiments. Butein (2.5 μM) was used as the positive control. $^{***}P < 0.001$ vs. LPS.

3.3.2. The effect of compounds 1-4 from *Fatsia japonica* on cell viability and nitrite reduction in BV2 cells.

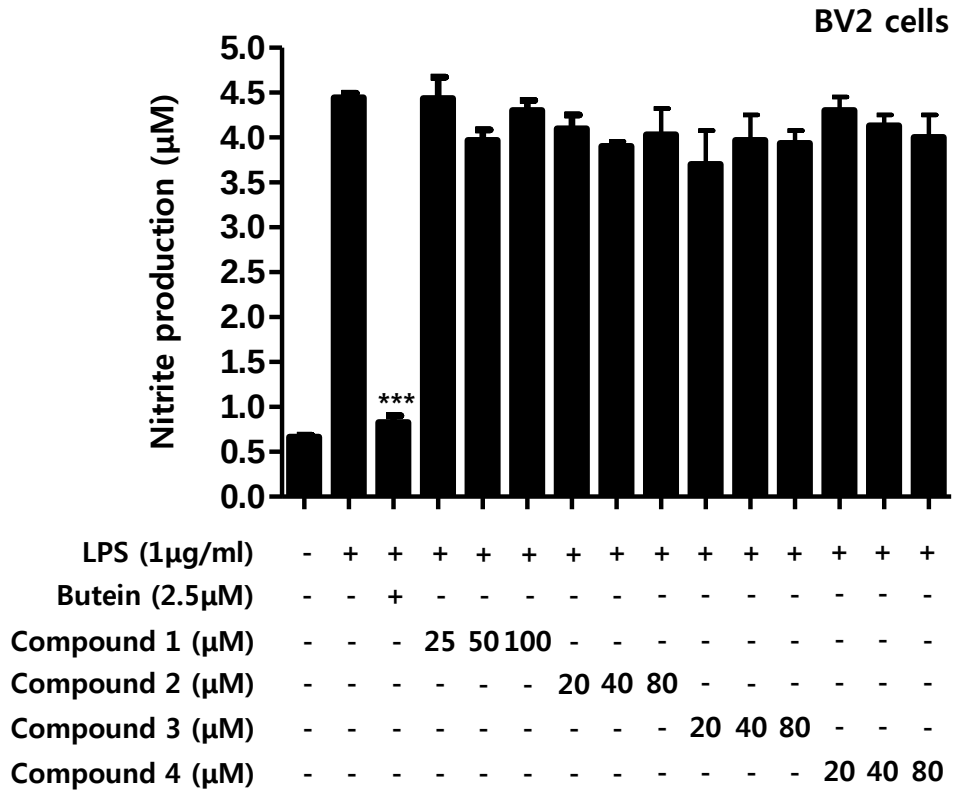

Fig. 20. The effects of compounds 1-4 from *Fatsia japonica* on nitrite reduction in BV2 cells. BV2 cells were treated with fractions from *Fatsia japonica* and then incubated for 24 h with LPS (1 μg/ml). Data are presented as mean ± SD values of 3 independent experiments. Butein (2.5 μM) was used as the positive control. $^{***}P < 0.001$ vs. LPS.

3.3.3. The effect of compounds 1-4 from *Fatsia japonica* on cell viability by MTT assay in HT22 cells.

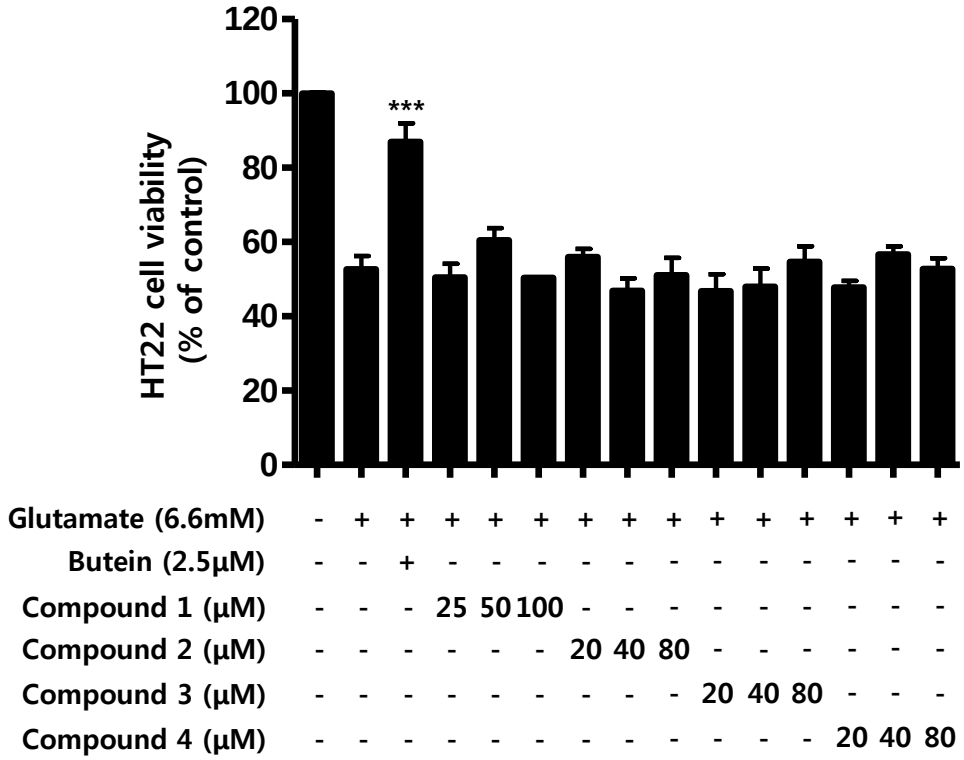

Fig. 21: The effects of compounds 1-4 from *Fatsia japonica* on cell viability by MTT assay in HT22 cells. HT22 cells were treated with fractions from *Fatsia japonica* and then incubated for 12 h with glutamate (5 mM). Data are presented as mean ± SD values of 3 independent experiments. Butein (2.5 μM) was used as the positive control. $^{***}P < 0.001$ vs. LPS.

4. Conclusion

F. japonica is grown wild to Eastern Asia, including Korea, Japan, and Taiwan and it is known as ornamental plant, and it is also known that pharmacological action through *F. japonica* leaf is effective for asthma, antitussive, expectorant, ache, gout and rheumatism and so on. The components of *F. japonica* leaves also reported to contain toxic compounds fatsia-sapotoxin, α-fatsin and β-fatsin. However, there are no studies about the anti-inflammatory, anti-neuroinflammatory, and neuro-protective actions of components from *F. japonica*. Characteristics of neurodegenerative diseases are related with nerve cell death and CNS inflammation. Prolonged inflammation can cause a variety of diseases including arthritis, neurodegenerative disorders, inflammatory bowel disease and septic shock syndrome. In addition, enormous inflammatory reactions cause the pathogenesis by interruption of tissue functions. In this thesis, on the beginning I have checked the screening of anti-inflammatory, anti-neuroinflammatory, and neuro-protective actions by using the extracts (47) and fractions (170) from 47 plants in Chosun University herb garden. Because, microglial activation and hippocampal cell death is one of the leading causes of neurodegenerative diseases. Next, I have selected the stem of *F. japonica* with consideration about biological activities and amount of yield. In addition, four compounds (**1**-**4**) were isolated from the stem of *F. japonica*. Extensive spectroscopic and chemical studies established the structures of these compounds as maltose (**1**), begoniifolide A (**2**), leiyemudanoside B (**3**), leonticin F (**4**). All of the compounds were investigated for their anti-inflammatory, anti-neuroinflammatory, and neuro-protective effects on RAW264.7, BV2, and HT22 cells. However, among four compounds, there were no effects by maltose (**1**), begoniifolide A (**2**), leiyemudanoside B (**3**), leonticin F (**4**) on the anti-inflammatory, anti-neuroinflammatory, and neuro-protective action. This is the first

report on the isolation of maltose (**1**), begoniifolide A (**2**), leiyemudanoside B (**3**), leonticin F (**4**) from the stem of *F. japonica*. In addition, the EtOH and *n*-BuOH fractions of *F. japonica* showed the anti-inflammatory, anti-neuroinflammatory, and neuro-protective actions, but the four isolated compounds from *n*-BuOH fraction of *F. japonica* didn't show any considerable anti-inflammatory, anti-neuroinflammatory, and neuro-protective effects. It might be necessary to continue the further studies to find the biological active compounds isolated from the stem of *F. japonica*. Because, the extracts and fractions from *F. japonica* have certainty effects on the anti-inflammatory, anti-neuroinflammatory, and neuro-protective action. This experiment suggests that *F. japonica* can treat neuronal cell death and neurodegenerative diseases caused by nitrite or glutamate. Furthermore, it can be considered that *F. japonica* can be used as a raw material for drugs for neurodegenerative diseases.

5. References

1. Lee, S.H., Kim, S.Y., Kim, D.W., Jang, S.H., Lim, S.S., Kwon, H.J., Kang, T.C., Won, M.H., Kang, I.J., Lee, K.S., Park, J., Eum, W.S., Choi, S.Y. (2008) Active component of *Fatsia japonica* enhances the transduction efficiency of Tat-SOD fusion protein both in vitro and in vivo. J Microbiol Biotechnol. (9):1613-9.

2. Lee, H.J., Lee, H.J., Yun, G.H., Lee, O.G., Kang, H.Y. (2006) *Fatsia japonica* extract components and physiological activity. Korean Society of Wood Science and Technology, < Journal of The Korean Wood Science & Technology > NO. 0:pp.272-273

3. TADASHI AOKI, YUMIKO TANIO and TAKAYIJKI SUGA (1976) TRITERPENOID SAPONINS FROM *Fatsia japonica*. Phytochcmistry, Vol. 15, pp. 781-784.

4. Kotake, M., Taguchi, K. and Okamoto, T. (1933) Rikagaku Kenkyusho Hbkoku 12, 590.

5. S Yu, X Ye, W Xin, K Xu, XY Lian, Z Zhang. (2014) Fatsioside A, a rare baccharane-type glycoside inhibiting the growth of glioma cells from the fruits of *fatsia japonica*. Planta Med; 80: 315–320

6. V. I. Grishkovets, E. A. Sobolev, A. S. Shashkov, V. Ya. Chirva. (2000) TRITERPENOID GLYCOSIDES OF *Fatsia japonica*. II. ISOLATION AND STRUCTURE OF GLYCOSIDES FROM THE LEAVES. Chemistry of Natural Compounds , Vol. 36, No. 5.

7. Wei Q, Qiu Z, Xu F, Li QR, Yin H. (2015) [Chemical Components from Leaves of *Fatsia japonica* and Their Antitumor Activities in vitro]. Zhong Yao Cai. 38(4):745-50.

8. http://www.cha.go.kr/korea/heritage/search/Culresult_Db_View.jsp?mc=NS_04_03_02&VdkVgwKey=16,00630000,38&queryText=&cultnm=%ED%86%B5%EC%98%81%20%EB%B9%84%EC%A7%84%EB%8F%84%20%ED%8C%94%EC%86%90%EC%9D%B4%EB%82%98%EB%AC%B4%20%EC%9E%90%EC%83%9D%EC%A7%80

9. S. K. Sonkusare et al., (2005) "Dementia of Alzheimer's disease and other neurodegenerative disorders-memantine, a new hope", Pharmacological Research, 51(1), pp.1-17.

10. P. Stanzione and D. Tropepi. (2011) "Drugs and clinical trials in neurodegenerative

diseases", Ann Ist Super Sanita, 47(1), pp.49-54, 2011.

11. Robert M. Friedlander, M.D. (2003) Apoptosis and Caspases in Neurodegenerative Diseases. N Engl J Med 348:1365-75
12. Träger U, Tabrizi SJ (2013) Peripheral inflammation in neurodegeneration[J]. J Mol Med, 91:673-681.
13. Yang Pan, Bo Shen, Qin Gao, Jun Zhu, Jingde Dong, Li Zhang2, Yingdong Zhang. (2016) Caspase-1 inhibition attenuates activation of BV2 microglia induced by LPS-treated RAW264.7 macrophages. J Biomed Res. 30(3):225-33.
14. Medzhitov, R. (2010) Inflammation 2010: New adventures of an old flame. Cell 140, 771–776.
15. Malyshev, I.Y., Shnyra, A. (2003) Controlled modulation of inflammatory, stress and apoptotic responses in macrophages. Curr. Drug Targets Immune Endocr. Metab. Disord. 3, 1–22.
16. Lynch, M.A. (2009) The multifaceted profile of activated microglia. Mol. Neurobiol. 40, 139–156.
17. Kim, K.J., Yoon, K.Y., Yoon, H.S., Oh, S.R., Lee, B.Y. (2015) Brazilein Suppresses Inflammation through Inactivation of IRAK4-NF- κ B Pathway in LPS-Induced Raw264.7 Macrophage Cells. Int. J. Mol. Sci. 16, 27589–27598.
18. Lipton SA, Rosenberg PA (1994) Excitatory amino acids as a final common pathway for neurologic disorders. N Engl J Med 330:613–622.
19. Gasic GP, Hollmann M (1992) Molecular neurobiology of glutamate receptors. Annu Rev Physiol 54:507–536.).
20. Difazio MC, Hollingsworth Z, Young AB, Penney JB Jr (1992) Glutamate receptors in the substantia nigra of Parkinson's disease brains. Neurology 42:402–406
21. Behrens PF, Franz P, Woodman B, Lindenberg KS, Landwehrmeyer GB (2002) Impaired glutamate transport and glutamate-glutamine cycling: downstream effects of the Huntington mutation. Brain 125:1908–1922.
22. Maher P, Davis JB (1996) The role of monoamine metabolism in oxidative glutamate

toxicity. J Neurosci 16:6394–6401

23. Halliwell B, Gutteridge JMC (1993) Free radicals in biology and medicine. Oxford University Press, New York

24. Mavelli I, Rigo A, Federico R, Ciriolo MR, Rotillo G (1982) Superoxide dismutase, glutathione peroxidase and catalase in the developing rat brain. Biochem J 204:535–540

25. Beynon SB, Walker FR (2012) Microglial activation in the injured and healthy brain: what are we really talking about? Practical and theoretical issues associated with the measurement of changes in microglial morphology. Neuroscience 225:162–171. doi:10.1016/j.neuroscience.2012.07.029

26. Lucin KM, Wyss-Coray T (2009) Immune activation in brain aging and neurodegeneration: too much or too little? Neuron 64:110–122. doi:10.1016/j.neuron.2009.08.039

27. Polazzi E, Monti B (2010) Microglia and neuroprotection: from in vitro studies to therapeutic applications. Prog Neurobiol 92:293–315. doi:10.1016/j.pneurobio.2010.06.009

28. Romero LI, Tatro JB, Field JA, Reichlin S (1996) Roles of IL-1 and TNF-α in endotoxin-induced activation of nitric oxide synthase in cultured rat brain cells. Am J Phys 270:326–332

29. Nakamura Y, Si QS, Kataoka K (1999) Lipopolysaccharide-induced microglial activation in culture: temporal profiles of morphological change and release of cytokines and nitric oxide. Neurosci Res 35:95–100. doi:10.1016/S0168-0102(99)00071-1

30. Fraschini C, Greffe L, Driguez H, Vignon MR (2005) Chemoenzymatic synthesis of 6omega -modified maltooligosaccharides from cyclodextrin derivatives. Carbohydr Res 340(11):1893-9.

31. Bekiroglu S, Kenne L, Sandström C (2003) 1H NMR studies of maltose, maltoheptaose, alpha-, beta-, and gamma-cyclodextrins, and complexes in aqueous solutions with hydroxy protons as structural probes. J Org Chem. 68(5):1671-8.

32. Roslund MU, Tähtinen P, Niemitz M, Sjöholm R. (2008) Complete assignments of the (1)H and (13)C chemical shifts and J(H,H) coupling constants in NMR spectra of D-glucopyranose and all D-glucopyranosyl-D-glucopyranosides. Carbohydr Res. 343(1):101-12.

33. Cioffi G, Dal Piaz F, Vassallo A, Venturella F, De Caprariis P, De Simone F, De Tommasi N (2008) Antiproliferative oleanane saponins from Meryta denhamii. J Nat Prod. 71(6):1000-4. doi: 10.1021/np8000464.

34. Li G, Zhang Y, Yang B, Xia Y, Zhang Y, Lü S, Kuang H (2010) Leiyemudanosides A-C, three new bidesmosidic triterpenoid saponins from the roots of Caulophyllum robustum. Fitoterapia. 81(3):200-4. doi: 10.1016/j.fitote.2009.08.025.

35. Wegner. C, Hamburger. M, Kunert. O, Haslinger. E (2000) Tensioactive compounds from the aquatic plant *Ranunculus fluitans* L. (Ranunculaceae). Helvetica Chimica Acta Vol.83 No.7 pp.1454-1464.

36. Chen M, Wu WW, Nanz D, Sticher O (1997) Leonticins D-H, five triterpene saponins from Leontice kiangnanensis. Phytochemistry. 44(3):497-504.

APPENDIX

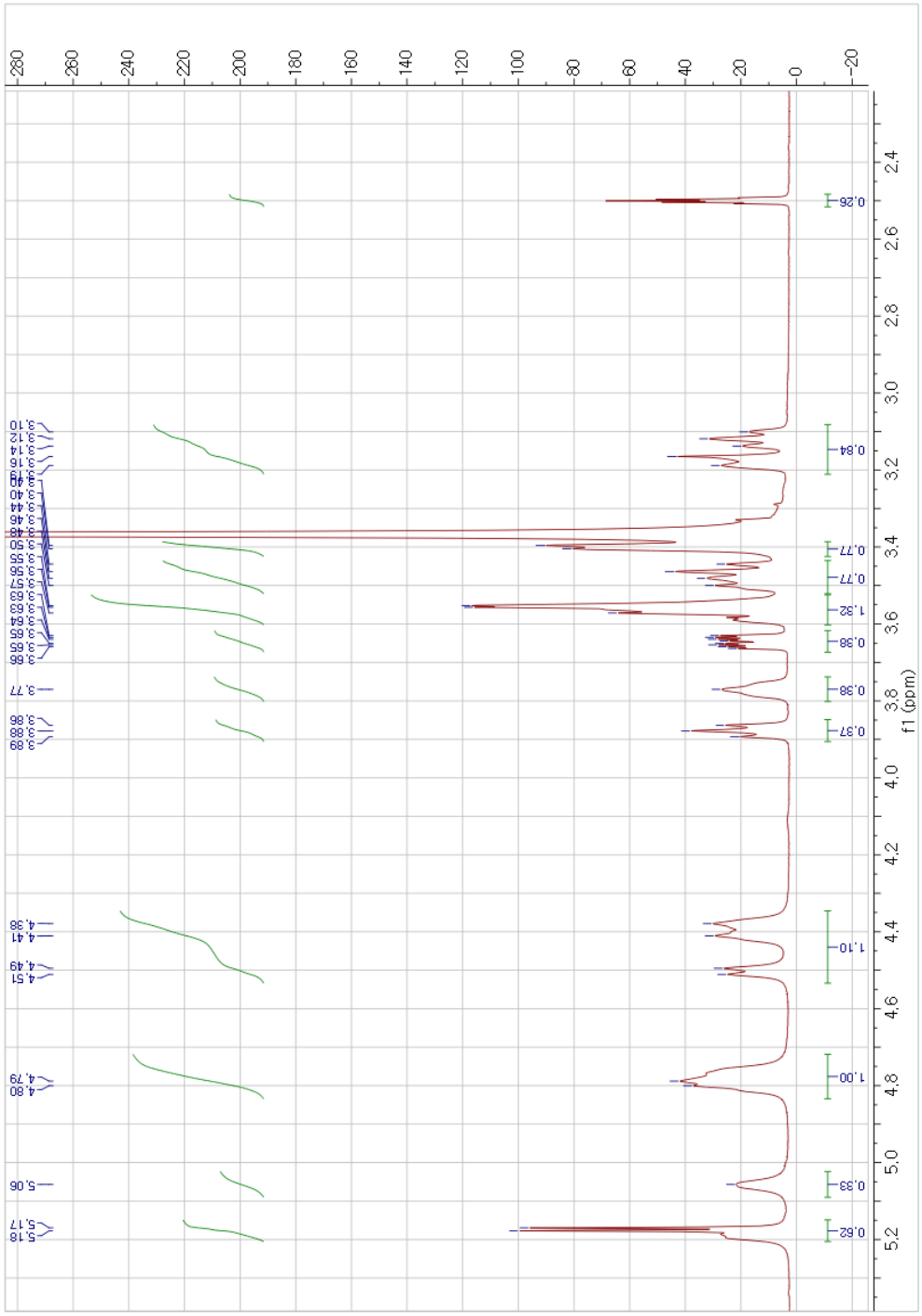

Fig.22: ^{1}H-NMR spectrum of compound 1 (500 MHz, DMSO-D_6)

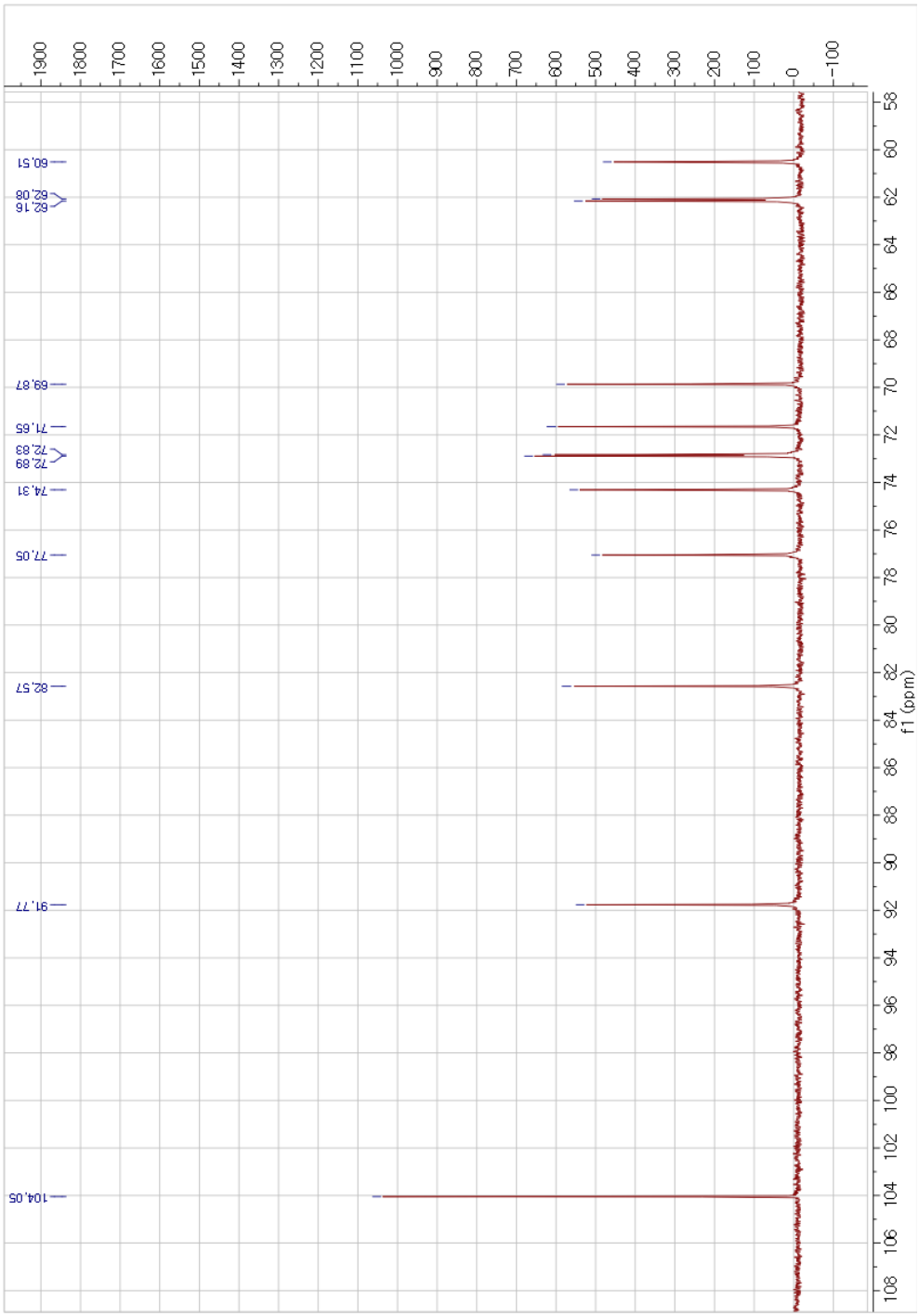

Fig. 23: ^{13}C-NMR spectrum of compound 1 (500 MHz, DMSO-D_6)

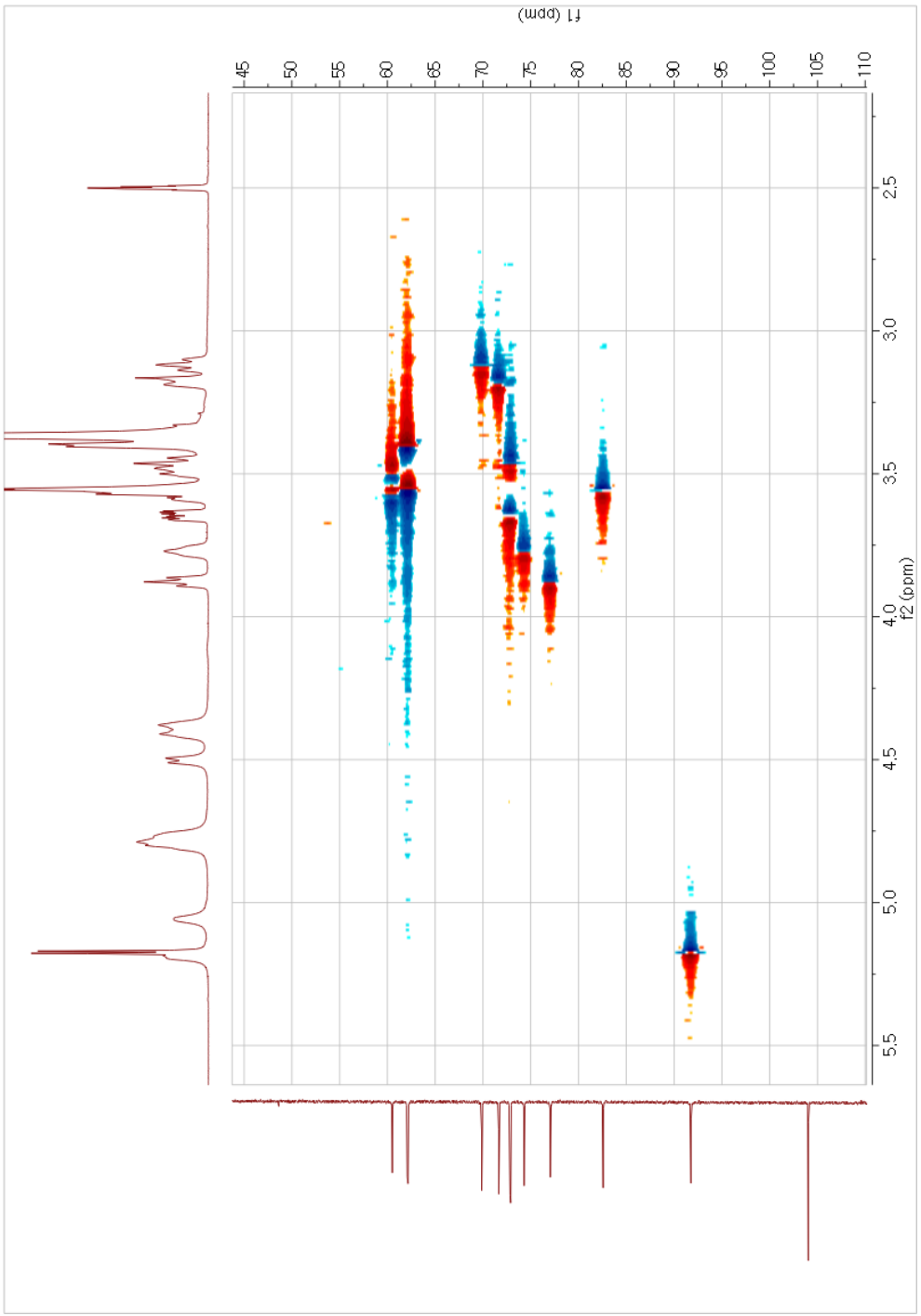

Fig.24: HSQC spectrum of compound 1 (500 MHz, DMSO-D_6)

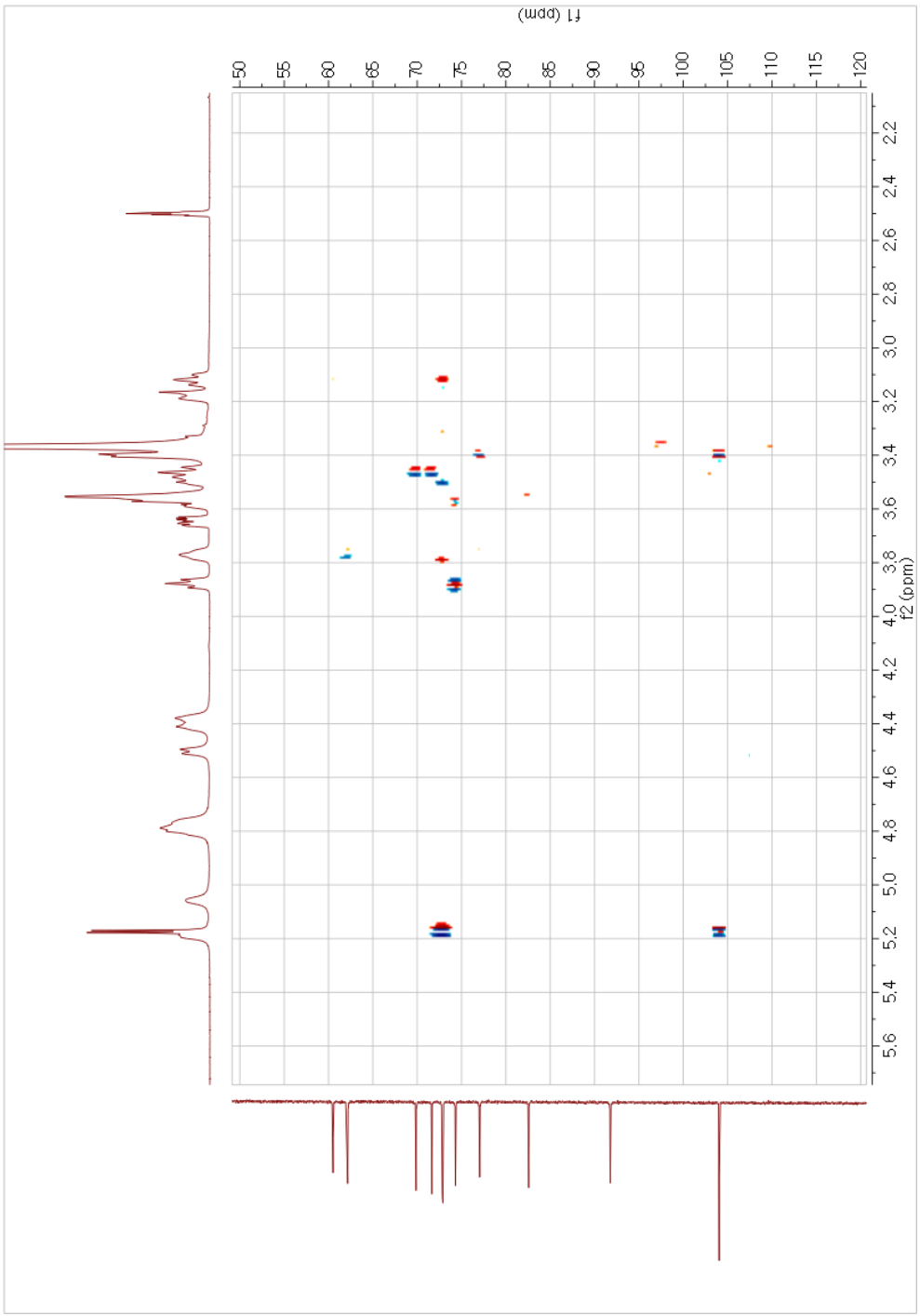

Fig.25: HMBC spectrum of compound 1 (500 MHz, DMSO-D_6)

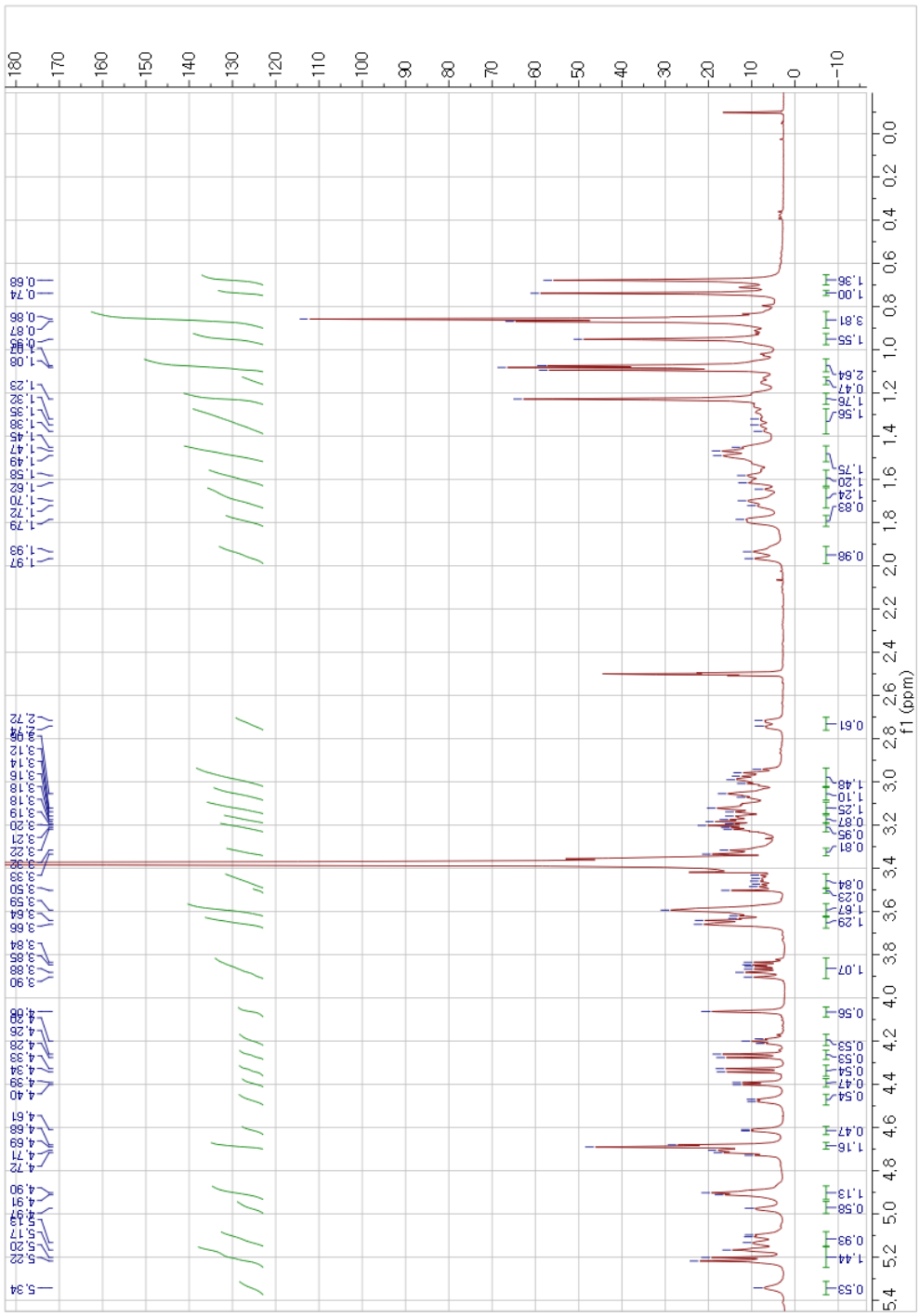

Fig.26: ^{1}H-NMR spectrum of compound 2 (500 MHz, DMSO-D_6)

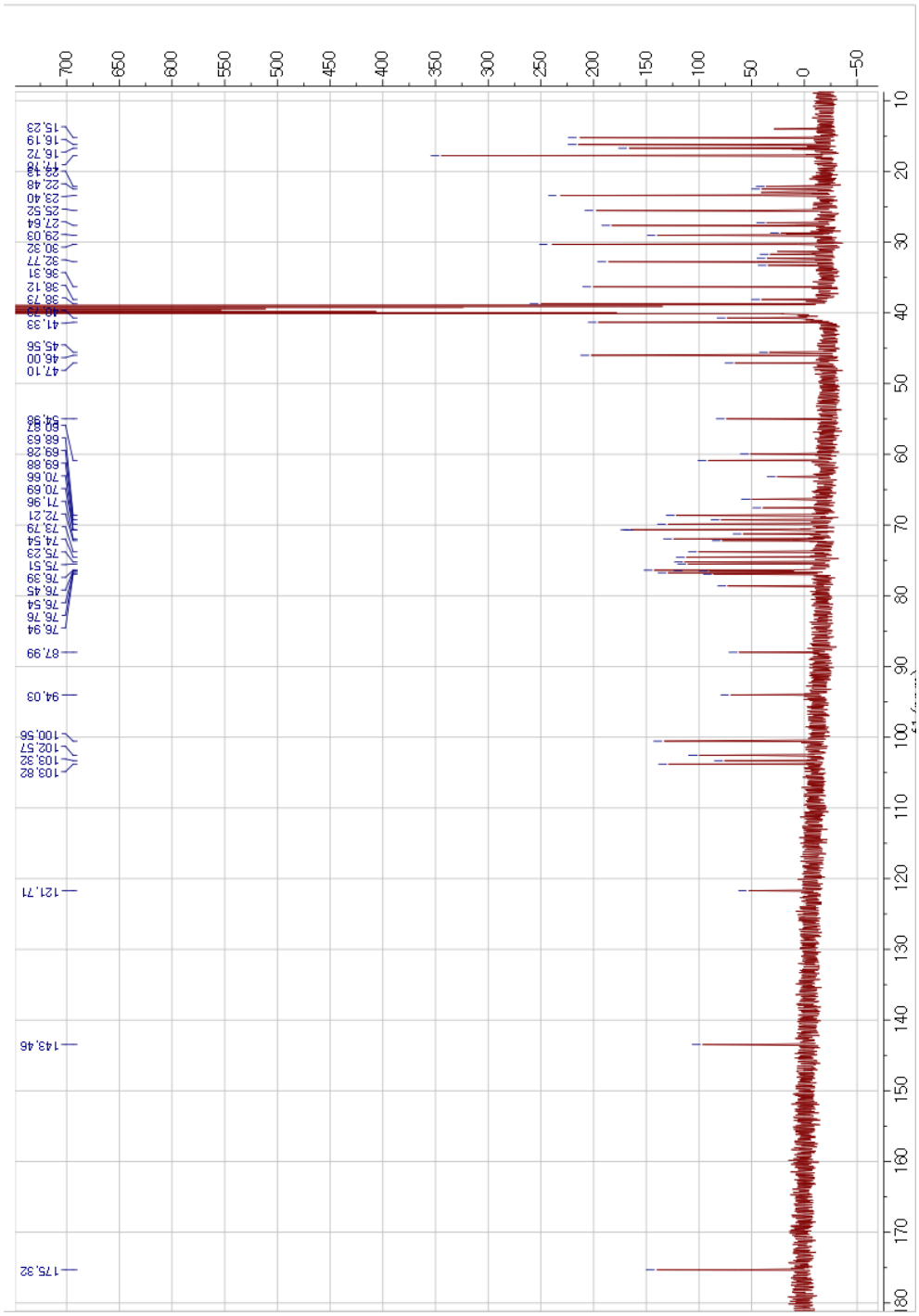

Fig..27: ^{13}C-NMR spectrum of compound 2 (500 MHz, DMSO-D$_6$)

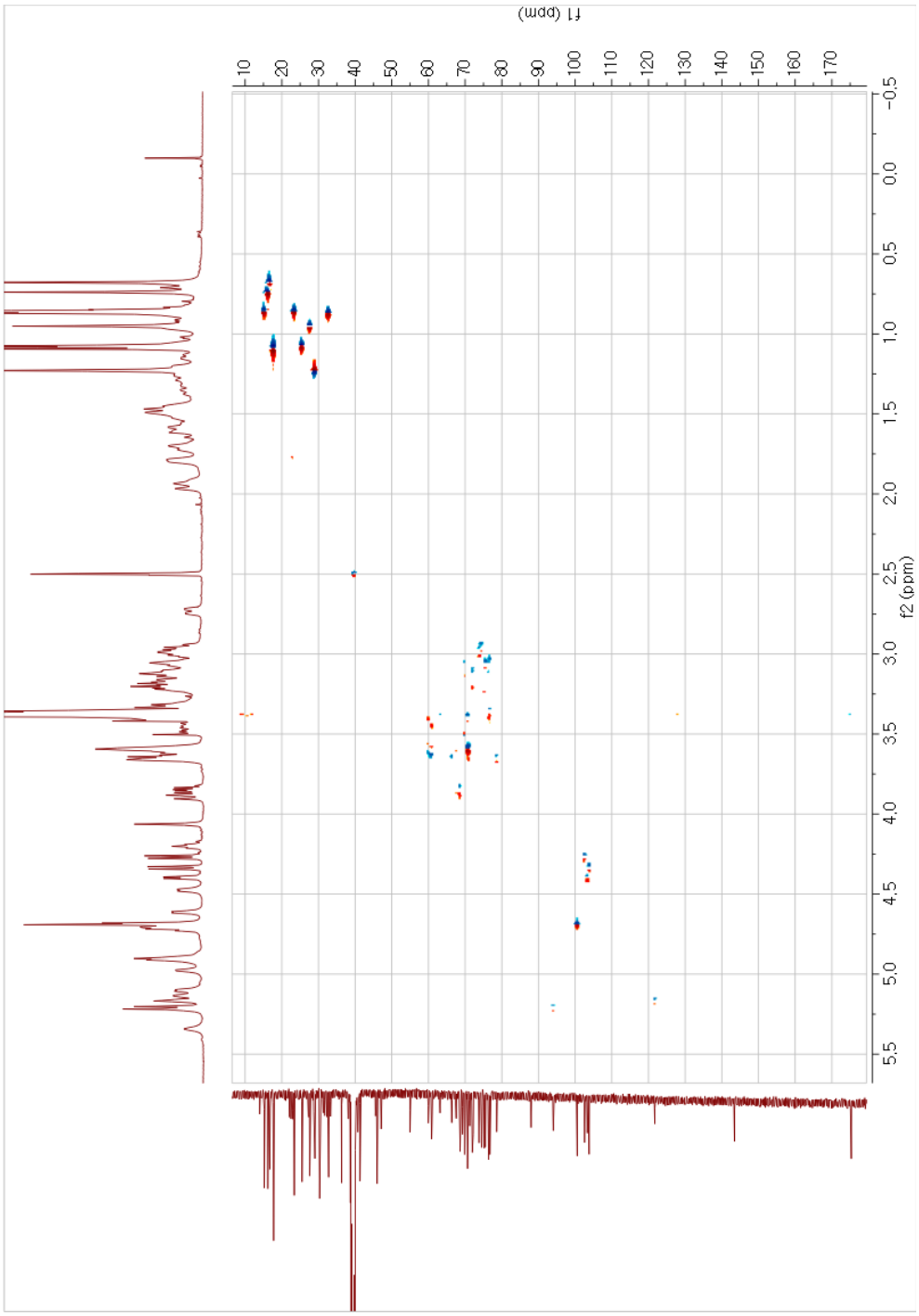

Fig.28: HSQC spectrum of compound 2 (500 MHz, DMSO-D_6)

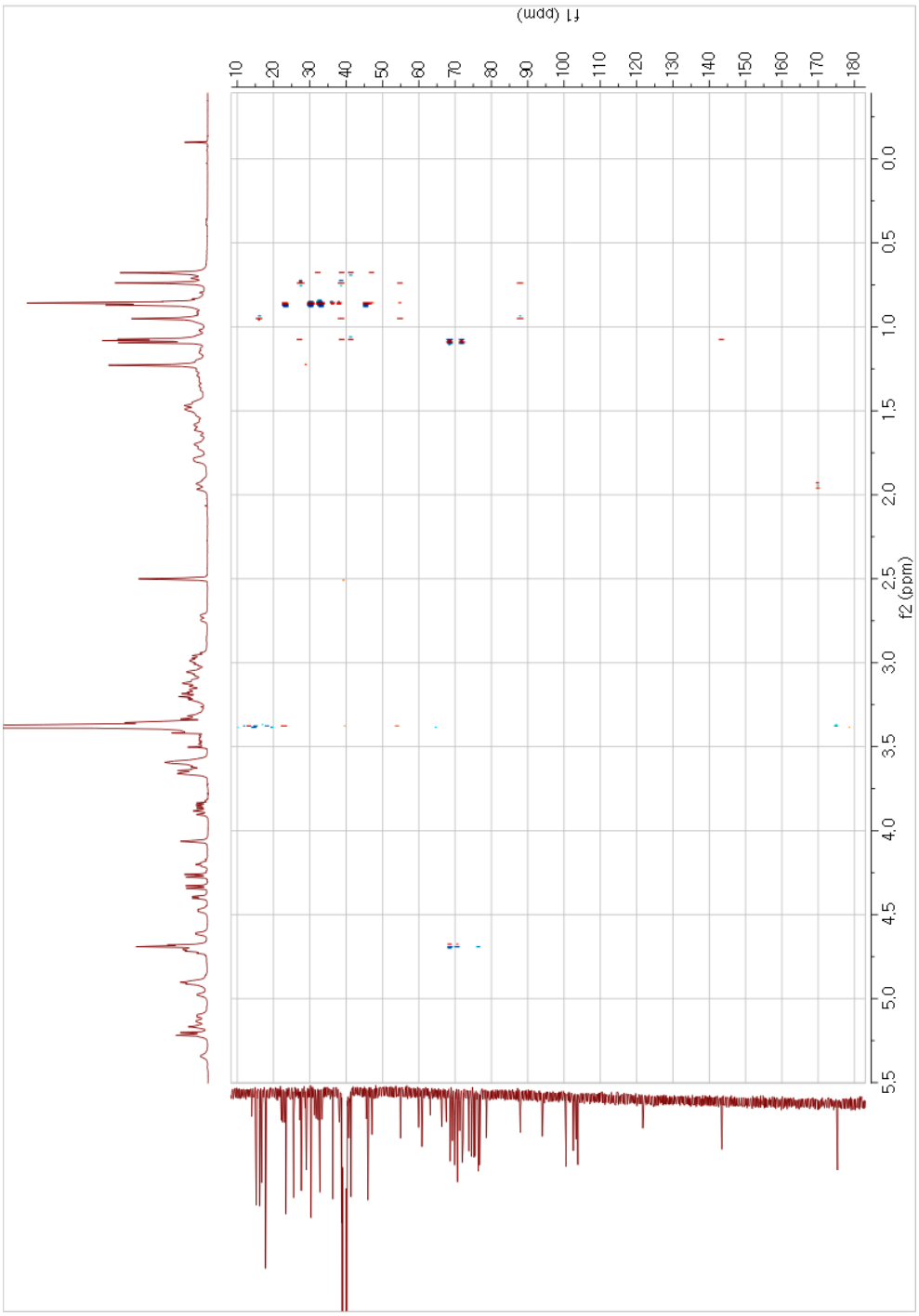

Fig.29: HMBC spectrum of compound 2 (500 MHz, DMSO-D_6)

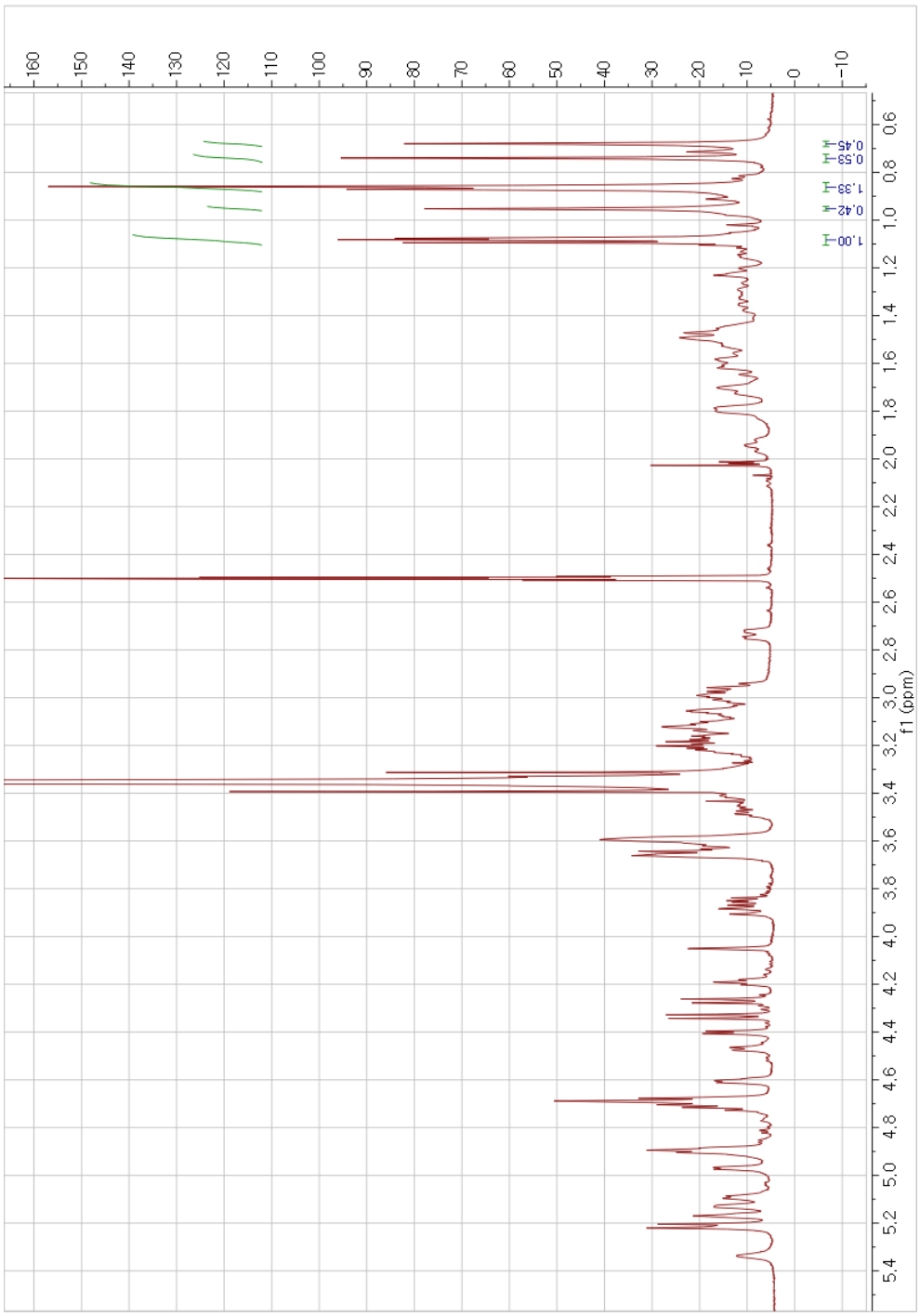

Fig.30: ^{1}H-NMR spectrum of compound 3 (500 MHz, DMSO-D_6)

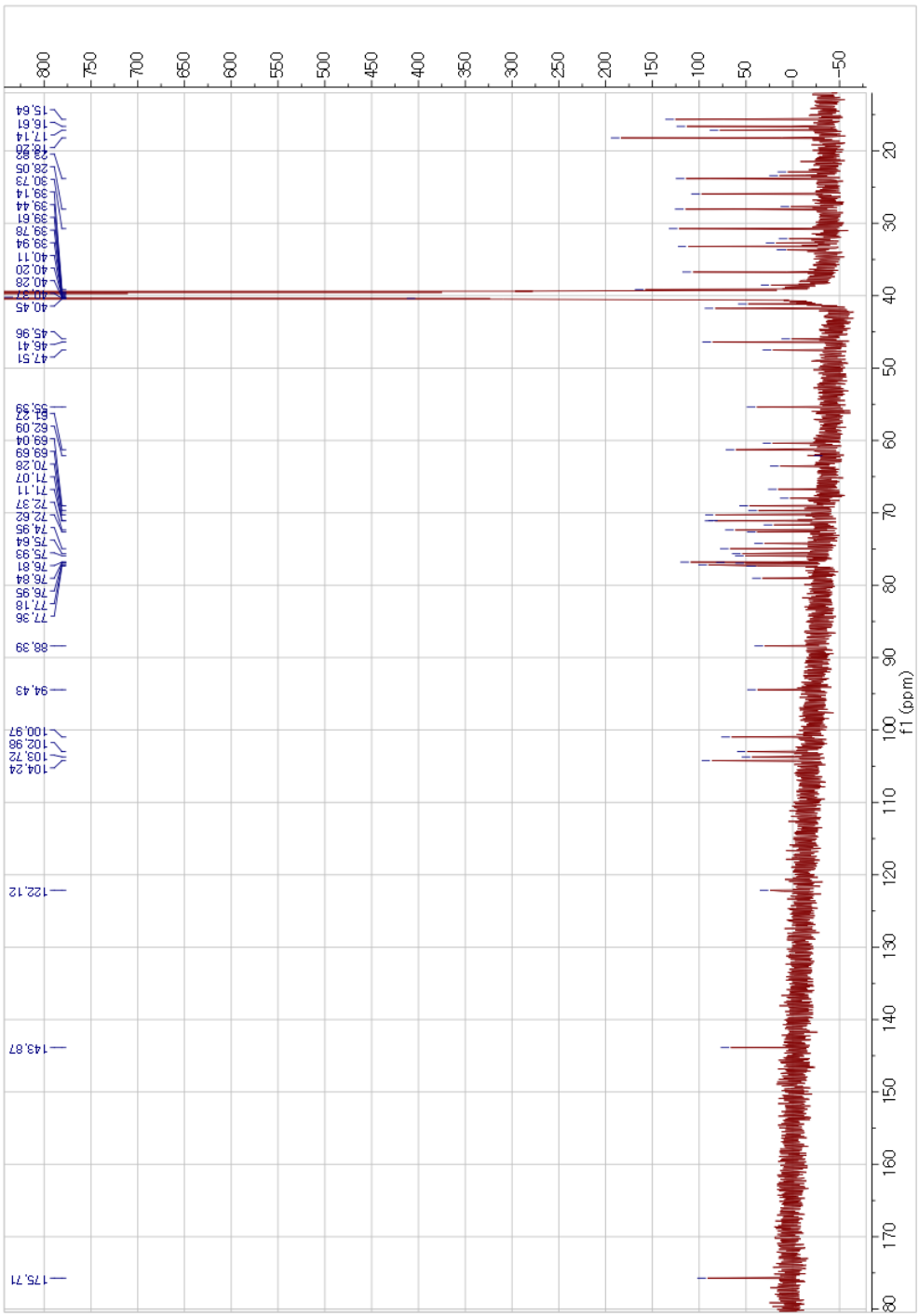

Fig.31: ^{13}C-NMR spectrum of compound 3 (500 MHz, DMSO-D_6)

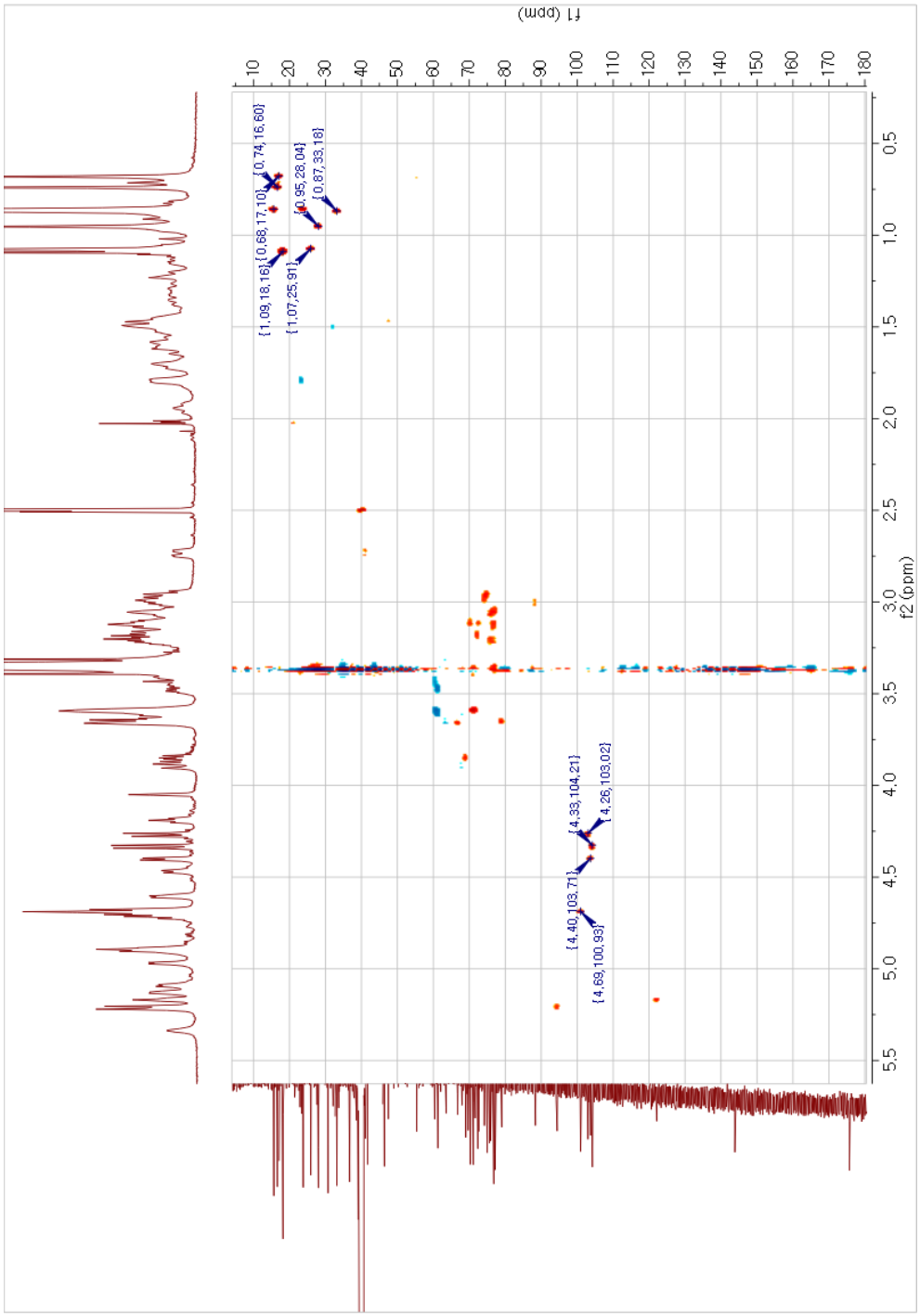

Fig.32: HSQC spectrum of compound 3 (500 MHz, DMSO-D_6)

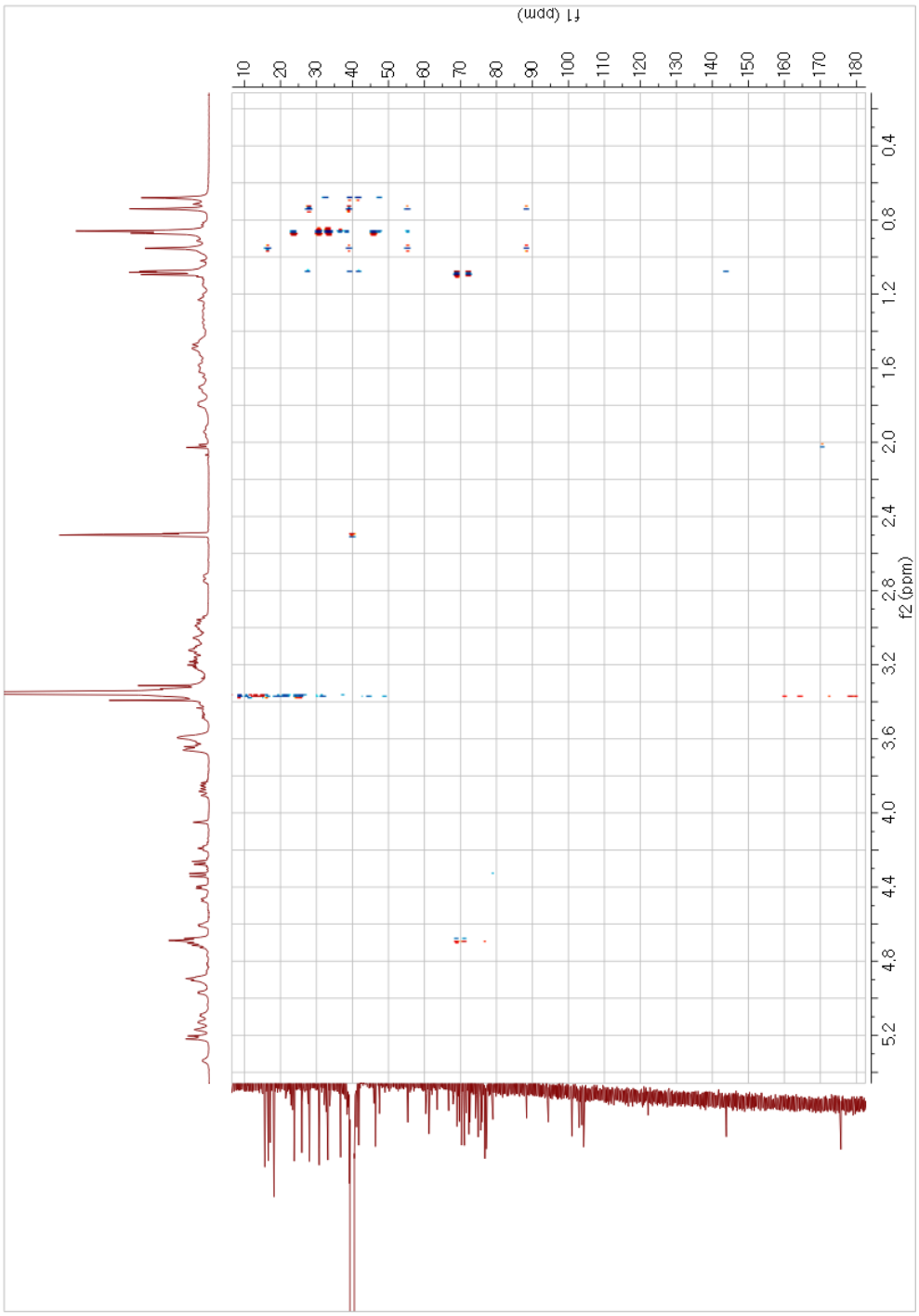

Fig.33: HMBC spectrum of compound 3 (500 MHz, DMSO-D_6)

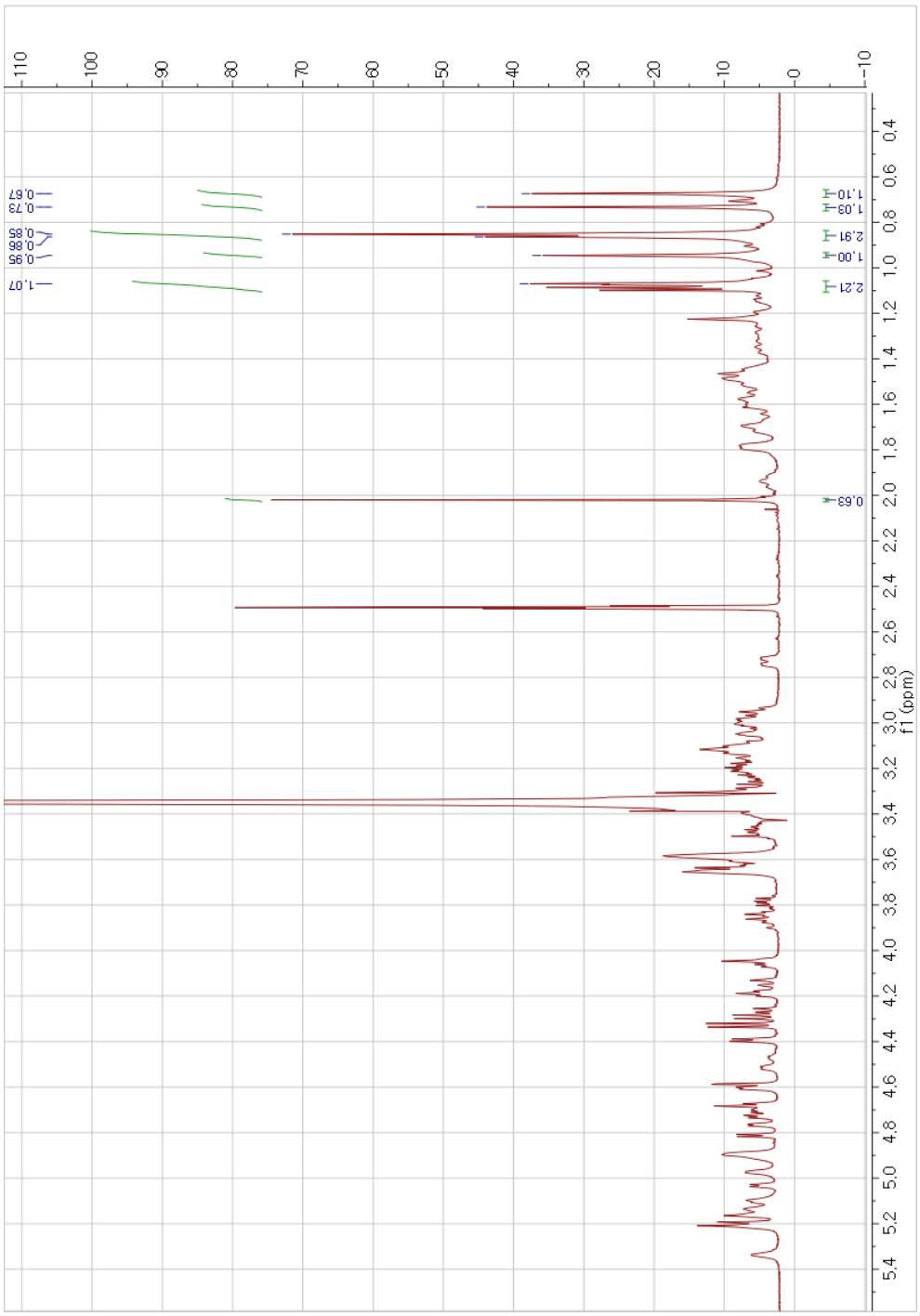

Fig.34: ^{1}H-NMR spectrum of compound 4 (500 MHz, DMSO-D_6)

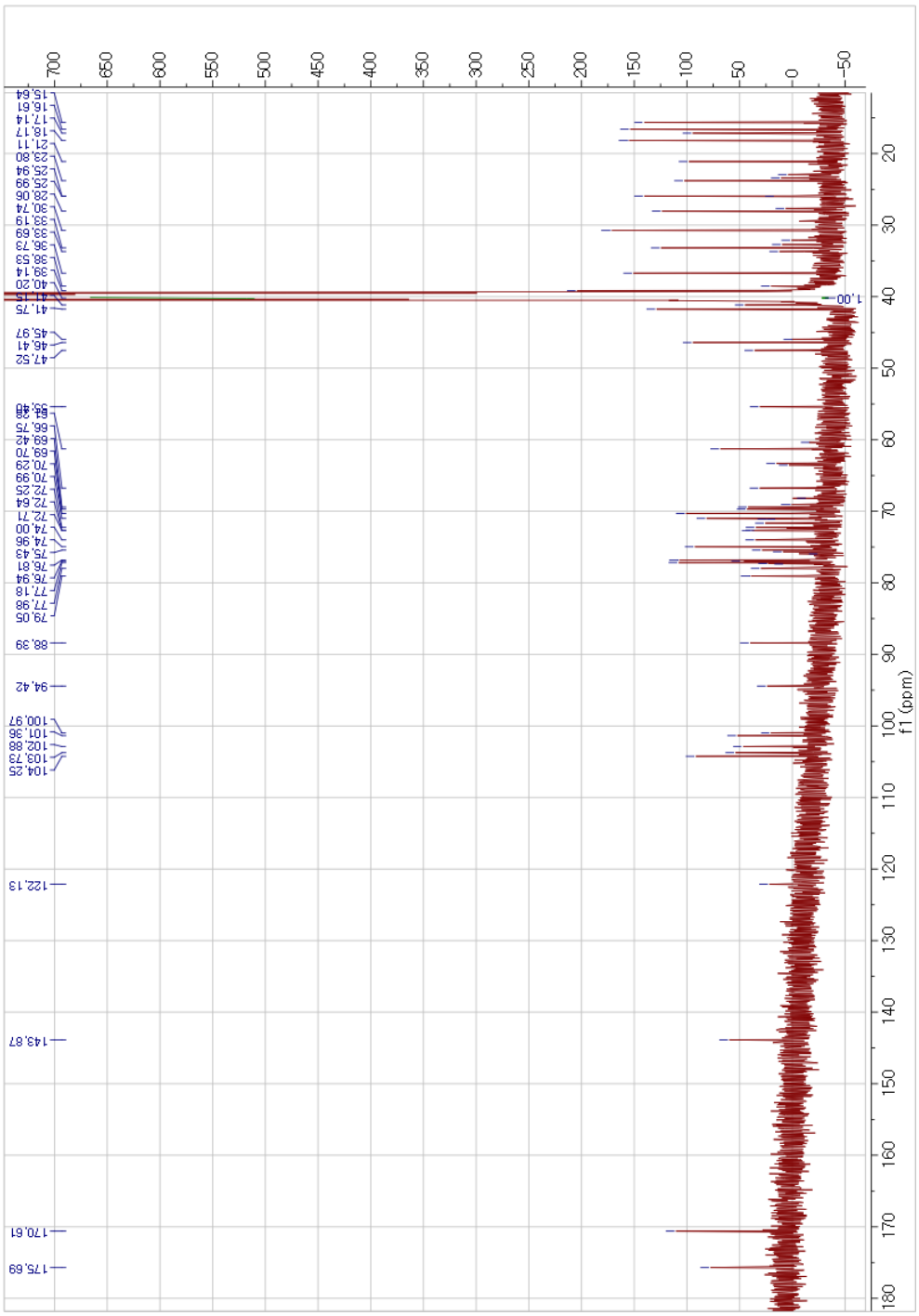

Fig..35: ^{13}C-NMR spectrum of compound 4 (500 MHz, DMSO-D_6)

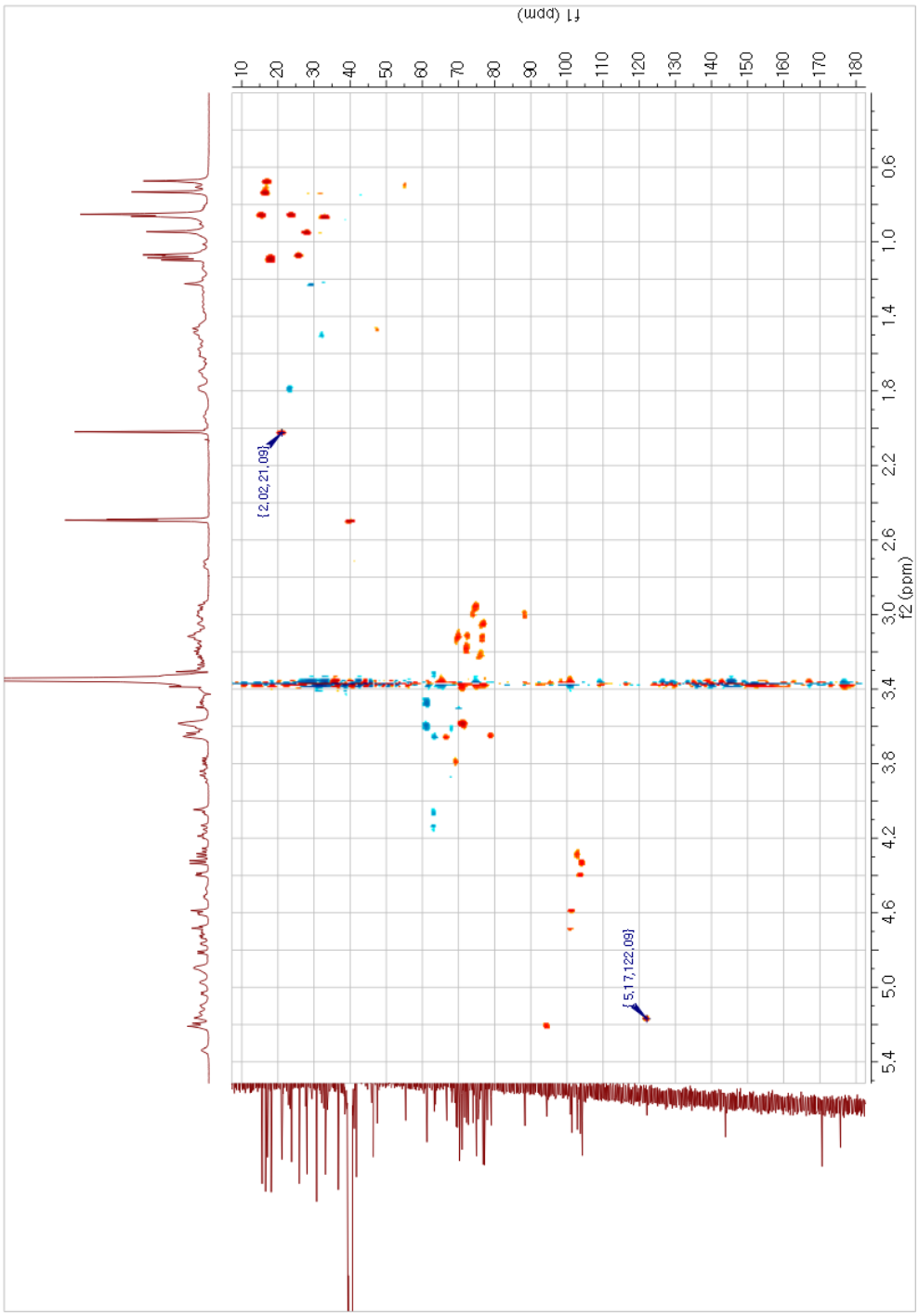

Fig.36: HSQC spectrum of compound 4 (500 MHz, DMSO-D_6)

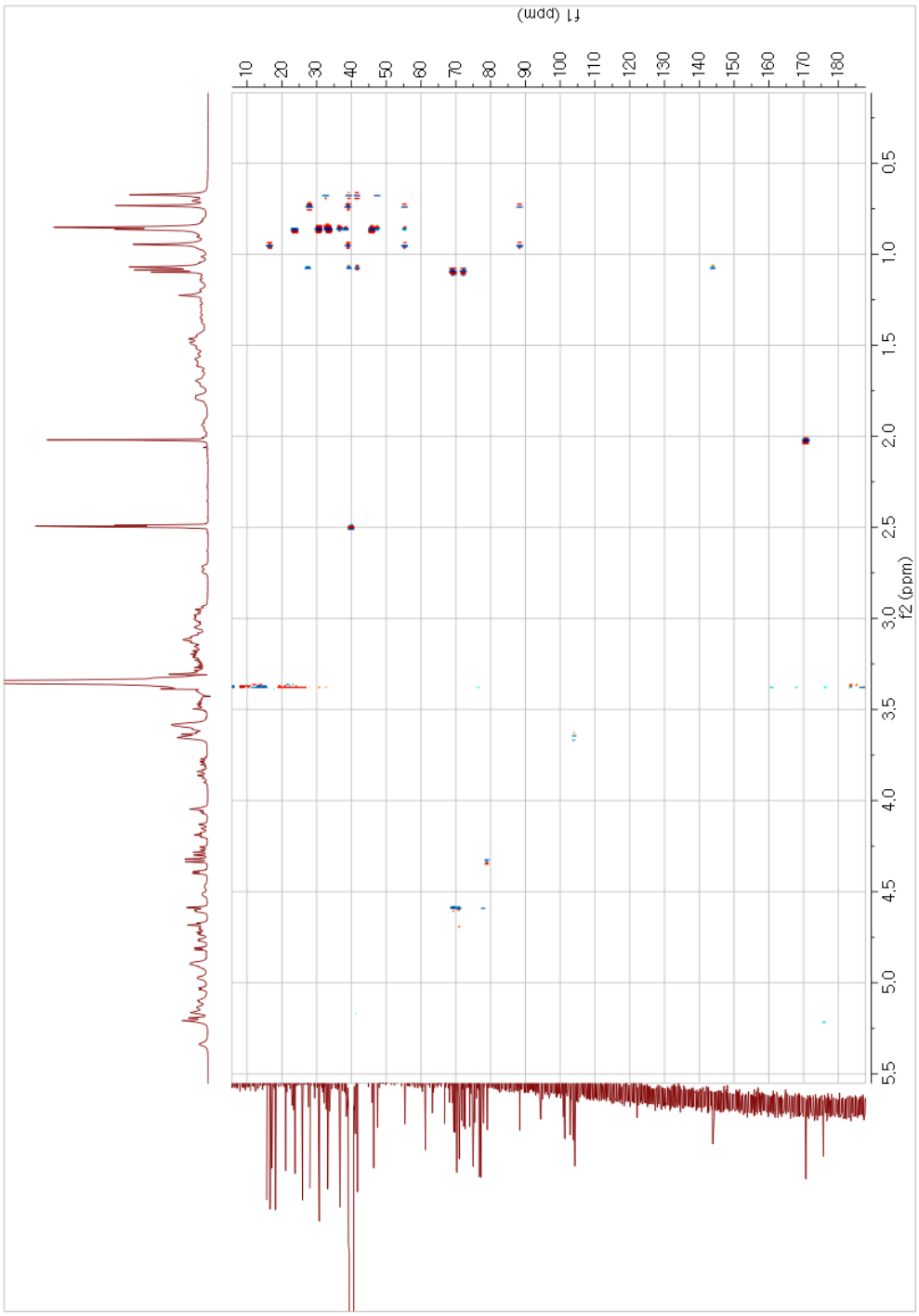

Fig.37: HMBC spectrum of compound 4 (500 MHz, DMSO-D_6)